iScience

Article

Trillin inhibits MAP3K11/NF-κB/COX-2 signaling pathways through upregulation of miR-145-5p in castration-resistant prostate cancer

Graphical abstract

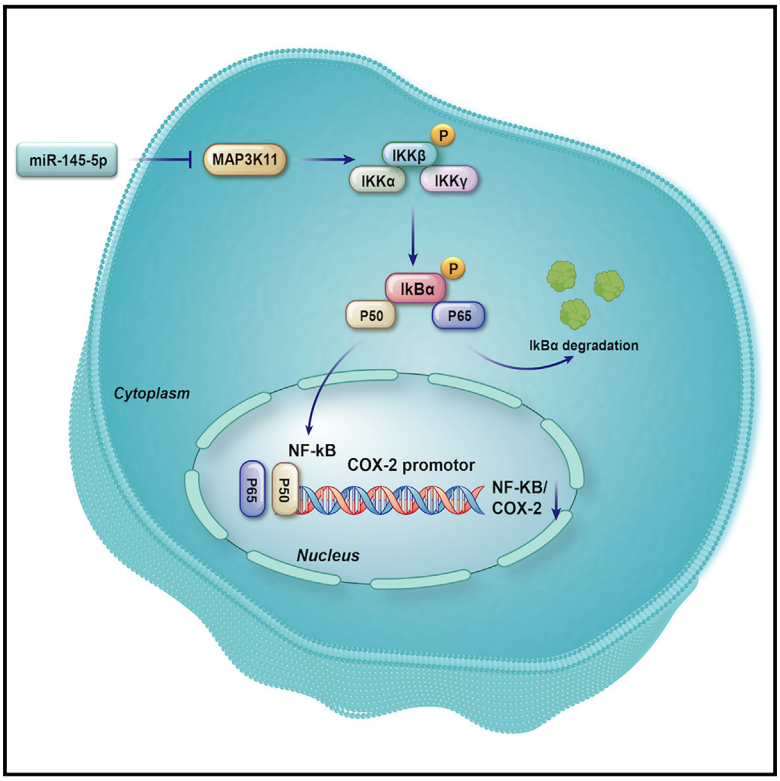

Authors

Yanlong Wang, Yulin Peng, Wenjun Hao, ..., Liang Wang, Zhenlong Yu, Zhiyu Liu

Correspondence

qdyuzl871123@163.com (Z.Y.), zyliu@dmu.edu.cn (Z.L.)

In brief

Cancer; Cell biology; Molecular biology

Highlights

- Upregulation of miR-145-5p suppresses CRPC cell proliferation and migration
- MAP3K11 was a downstream target of miR-145-5p
- Trillin enhances miR-145-5p levels, demonstrating potential as a CRPC therapy

Wang et al., 2025, iScience *28*, 111505
February 21, 2025 © 2024 Published by Elsevier Inc.
https://doi.org/10.1016/j.isci.2024.111505

CellPress

iScience

CellPress
OPEN ACCESS

Article

Trillin inhibits MAP3K11/NF-κB/COX-2 signaling pathways through upregulation of miR-145-5p in castration-resistant prostate cancer

Yanlong Wang,[1,4] Yulin Peng,[2,4] Wenjun Hao,[1,4] Chengjian He,[2,4] Xiang Gao,[1] Peng Liang,[1] Haolin Zhao,[1] Ying Wang,[1] Liang Wang,[1] Zhenlong Yu,[2,*] and Zhiyu Liu[3,5,*]

[1]Department of Urology, The Second Hospital of Dalian Medical University, Dalian 116023, China
[2]College of Integrative Medicine, College of Pharmacy, Dalian Medical University, Dalian 116044, China
[3]Department of Urology, The Second Hospital of Dalian Medical University, Liaoning Provincial Key Laboratory of Urological Digital Precision Diagnosis and Treatment, Liaoning Engineering Research Center of Integrated Precision Diagnosis and Treatment Technology for Urological Cancer, Dalian Key Laboratory of Prostate Cancer Research, Dalian 116023, China
[4]These authors contributed equally
[5]Lead contact
*Correspondence: qdyuzl871123@163.com (Z.Y.), zyliu@dmu.edu.cn (Z.L.)
https://doi.org/10.1016/j.isci.2024.111505

SUMMARY

Castration-resistant prostate cancer (CRPC) presents a significant challenge in treatment following androgen deprivation therapy. This study evaluates Trillin, a compound with antioxidant and anti-inflammatory properties, for its therapeutic potential against CRPC. Using DU145 and PC3 cell lines and a mouse xenograft model, we demonstrate that Trillin effectively inhibits CRPC cell viability, proliferation, migration, and invasion while promoting apoptosis and cell-cycle arrest. Mechanistic investigations reveal that Trillin disrupts NF-κB/COX-2 signaling by downregulating MAP3K11 and COX-2 and inhibiting the nuclear translocation of NF-κB subunits. Additionally, Trillin enhances the expression of miR-145-5p, further modulating pathways critical for CRPC progression. These findings suggest that Trillin may offer a promising alternative approach for targeting CRPC, highlighting its potential as a therapeutic agent to improve patient outcomes.

INTRODUCTION

Prostate cancer (PCa) is a prevalent malignancy in men, with an estimated 288,300 new cases in the United States in 2023, making it the most common cancer among men and resulting in approximately 34,700 deaths, thus ranking second in male cancer mortality.[1] In China, although the global incidence and mortality rates of prostate cancer are relatively low, there has been a significant rise, with the age-standardized incidence rate reaching 17.3 per 100,000 in 2019, a 95.2% increase since 1990, leading to roughly 50,000 deaths.[2] While early-stage prostate cancer usually responds well to androgen deprivation therapy (ADT), resistance often develops, progressing to more aggressive castration-resistant prostate cancer (CRPC).[3,4] Current research on PCa primarily focuses on the prevention and treatment of CRPC, including chemotherapeutic drugs, hormone inhibitors, and tumor vaccines.[5–7] Nevertheless, these therapies frequently entail severe adverse effects, underscoring the imperative to identify low-toxicity approaches for managing CRPC.[8]

Inflammation, which is recognized as a crucial aspect of cancer development,[9] plays a significant role in the initiation and progression of PCa, primarily through alterations in the tumor microenvironment. A notable example is the impact of inflammation on the transition of PCa to CRPC.[10] Massive research indicates that senescence-related myeloid inflammation not only accelerates the metastasis of CRPC but also undermines the efficacy of treatments targeting the androgen receptor.[11] Central to these inflammatory processes is the nuclear factor-kappa B (NF-κB) pathway, identified as a key player in the progression of prostate cancer to CRPC.[12] The role of cyclooxygenase-2 (COX-2) playing in exacerbating prostate cancer and facilitating the emergence of CRPC is well-documented, with studies showing its high expression as a contributing factor.[13] COX-2 expression is intricately regulated by transactivators such as NF-κB.[14] Interestingly, inhibiting COX-2 through immunoproteasome intervention has shown promise in preventing the development of CRPC.[15] Therefore, strategies focusing on the NF-κB/COX-2 axis could be instrumental in enhancing the treatment outcomes for CRPC.[16]

MicroRNAs (miRNAs) are definitely the crucial non-coding RNA molecules in cancer research, significantly involved in regulating tumorigenesis, cell proliferation, differentiation, and apoptosis.[17] Among these miRNAs, miR-145 plays a pivotal role in regulating numerous oncogenes and diverse cellular processes such as inflammation.[18,19] This modulation is instrumental in the progression of PCa from a localized to a metastaticstate.[20] In the context of CRPC, miRNAs are increasingly recognized as vital epigenetic regulators and promising

This is an open access article under the CC BY-NC-ND license (http://creativecommons.org/licenses/by-nc-nd/4.0/).

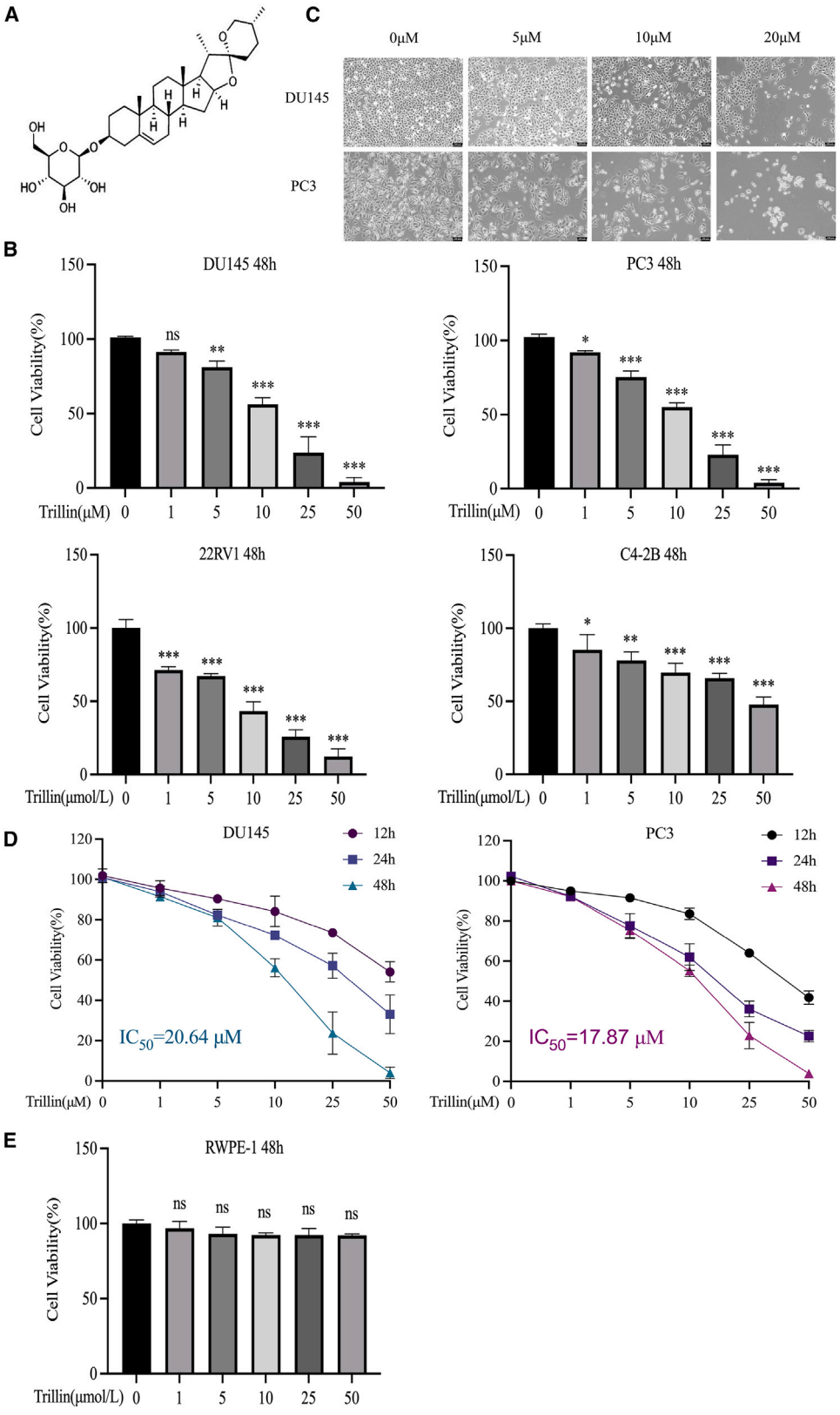

(legend on next page)

biomarkers,[21] opening up fresh possibilities for therapeutic interventions.[22] Notably, miR-30c-1-3p and miR-103a-2-5p, which are downregulated in CRPC, have been identified as tumor suppressors.[23] Deep sequencing comparisons of miRNA expressions in metastatic CRPC (mCRPC), non-PCa, and hormone-sensitive prostate cancer (HSPC) specimens have identified miR-145-5p as the most downregulated, underscoring its tumor-suppressing impact in CRPC.[24] In addition, the plasma expression levels of miR-145-5p were observed to be downregulated in mCRPC patients compared to control groups, consistent with the reported downregulation of this miRNA in prostate cancer tissue.[25] Further studies using small RNA sequencing have elucidated the role of miR-145-5p in CRPC, particularly its dysregulated expression and tumor-suppressing function through targeting genes such as c-MYC and CDKN1A.[26] However, a comprehensive understanding of the specific role of miR-145-5p in CRPC necessitates further research.

Trillium tschonoskii maxim (TTM) is a traditional Chinese medicine extensively utilized in China to treat conditions such as hypertension, headaches, and inflammation.[27] Trillin (Figure 1A), an extract from TTM, has gained widespread attention for its documented anticancer properties. Previous studies have demonstrated Trillin's ability to inhibit autophagy, induce apoptosis in hepatocellular carcinoma cells, reduce invasion, and hinder tumor growth.[28,29] Furthermore, it has exhibited notable effects in arresting mitosis in leukemia cells.[30] Nonetheless, the precise mechanism by which Trillin acts on CRPC cells, particularly its potential to downregulate NF-κB/COX-2 expression and suppress cancer cell proliferation, remains insufficiently explored. This investigation aims to assess the therapeutic potential of Trillin in addressing CRPC and elucidate its underlying mechanisms, potentially paving the way for original CRPC treatment strategies.

RESULTS

Trillin-induced inhibition of proliferation and cellular morphology alterations in CRPC cells

To evaluate Trillin's impact on CRPC, we examined its effects on the proliferation of AR-negative CRPC cells (DU145 and PC3) and AR-positive CRPC cells (22RV1 and C4-2B). As shown in Figure 1B, Trillin exhibited similar inhibitory effects on the viability of both AR-positive cells and AR-negative CRPC cells, demonstrating its broad-spectrum efficacy against various CRPC cell models. Therefore, we selected DU145 and PC3 cells for further investigation into the mechanism of Trillin's anti-CRPC effects. The results showed that Trillin increased the contraction and membrane blebbing of CRPC cells (Figure 1C) and also resulted in time- and dose-dependent inhibition of proliferation (Figure 1D). The half-maximal inhibitory concentration (IC_{50}) for Trillin was determined to be 20.64 ± 1.79 μM for DU145, and 17.87 ± 3.17 μM for PC3 cells over 48 h, as depicted in Figure 1D.

In addition, we also accessed the effects of Trillin on non-malignant prostate epithelial cell line RWPE-1. The results indicate that Trillin has minimal toxicity on RWPE-1 cells. These findings suggest that Trillin does not exhibit significant toxicity toward normal prostate epithelial cells (Figure 1E), further supporting its potential as a safe therapeutic agent.

Trillin-mediated inhibition of colony formation and cellular cycle in CRPC cells

A colony formation assay was performed to evaluate the influence of Trillin on the clonogenic potential of both DU145 and PC3 cells. The results presented in Figure 2A reveal that Trillin treatment resulted in a significant reduction in colony formation, led to a noticeable decline in the colony formation ratio. It is recognized that the inhibition of cell proliferation is intricately linked with changes in the progression of the cell cycle.[31] Therefore, the effects of Trillin on cell cycle progression were also examined. Trillin treatment significantly increased in the percentage of cells in the G0/G1 phase, increasing from 43.1% to 65.4% in DU145 cells, and from 42.1% to 65.0% in PC3 cells.

Additionally, a decrease in the G2/M phase was observed, decreasing from 29.3% to 15.9% and from 22.6% to 15.8%, respectively (Figure 2B). These findings indicate that Trillin inhibits the proliferation of DU145 and PC3 cells by inducing cell-cycle arrest at the G0/G1 phase. To further elucidate the molecular mechanisms underlying Trillin-induced cell-cycle arrest, the expression of key cell cycle-related proteins such as CDK4 and cyclin D1 was analyzed through western blot (Figure 2C). The reduced expression of these proteins may be associated with the observed cell-cycle arrest.

Trillin-mediated inhibition of migration and invasion in CRPC cells

Wound healing and transwell assays were additionally utilized to assess the influence of Trillin on cell migration and invasion in CRPC cells. Trillin treatment resulted illustrated in Figures 3A and 3B in a notable decrease in the migration and invasion capabilities of both DU145 and PC3 cells in a dose-dependent manner. Additionally, the evaluation of key proteins associated with these processes revealed notable changes in their expression. Specifically, Trillin resulted in a notable reduction in MMP-2, MMP-9, and N-cadherin levels, while promoting the

Figure 1. Trillin suppresses viability and alters morphology of CRPC cells

(A) Chemical structure of Trillin.

(B) AR-negative CRPC cells (DU145 and PC3) and AR-positive CRPC cells (22RV1 and LNCaP C4-2B) were subjected to different concentrations of Trillin for a 48-h duration, and cell viability was quantified through the CCK-8 assay.

(C) Morphological alterations and decreased proliferation in DU145 and PC3 cells following 48 h of Trillin treatment. Scale bar: 100 μm.

(D) Effect of Trillin on DU145 and PC3 cells on cell survival in a manner dependent on both concentration and time. Following treatment with Trillin for 48 h, CCK-8 assay assessed IC_{50} values.

(E) CCK-8 assay detects the effect of Trillin on the non-malignant prostate epithelial cell line RWPE-1. The results were calculated from three independent experiments. (Data were statistically analyzed with one way ANOVA and value was shown as mean ± SD of 3 independent experiments; ns indicates not significant; $^{*}p < 0.05$; $^{**}p < 0.01$; $^{***}p < 0.001$).

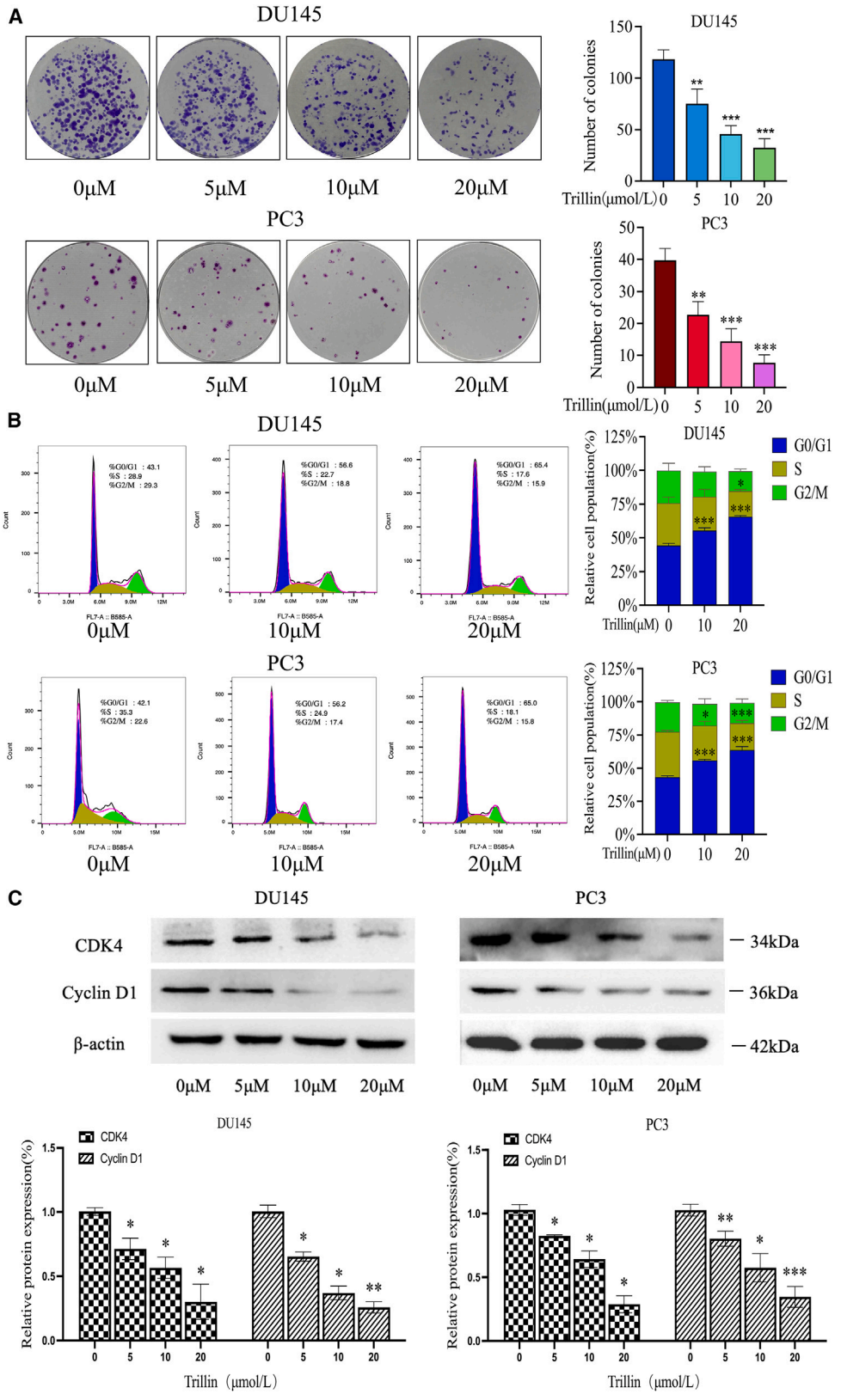

(legend on next page)

expression of E-cadherin (Figure 3C). These findings demonstrate that Trillin effectively inhibits the migration and invasion capabilities of CRPC cells.

Trillin-mediated apoptosis in CRPC cells through the mitochondrial pathway

Trillin treatment in this study led to a noticeable, dose-dependent increase in apoptosis in DU145 and PC3 cells (Figure 4A). To investigate the underlying mechanisms of Trillin-induced apoptosis, a comprehensive assessment of pro- and anti-apoptotic proteins was conducted using western blot analysis. This analysis covered caspase-3/9 and cleaved caspase-3/9, PARP and cleaved PARP, Bax and Bcl-2 in both cell lines. The results indicated that Trillin treatment significantly elevated the levels of cleaved caspase-3, caspase-9, cleaved PARP, and Bax, while reducing Bcl-2 expression compared to the control group (Figure 4B).

Moreover, immunofluorescence imaging (IFI) analysis was used to observe the effect of Trillin on the release of cytochrome *c* (cyto *c*). Trillin significantly triggers the release of cyto *c* from the inter-mitochondrial space into the cytosol of CRPC cells (Figure 5A). Meanwhile, Western blot analysis also confirmed that cyto *c* expression increased with increasing doses of Trillin (Figure 5B). To ensure that the observed effects were not due to changes in the amount of mitochondria, western blot of voltage-dependent anion channel-1 (VDAC-1) was performed, which showed no significant changes in mitochondrial quantity due to Trillin treatment. Based on these observations, the study concludes that Trillin can trigger apoptosis in CRPC cells by initiating the release of cyto *c*, which in turn promotes the activation of various caspase cascades in the cytosol, contributing to its pro-apoptotic effects.

Trillin-induced inhibition of COX-2 and NF-κB expression in CRPC cells

High expression of COX-2 is a known contributor to cancer cell proliferation, migration, and invasion.[32–34] Interestingly, Trillin, a compound previously recognized for its anti-inflammatory and anti-fibrotic properties,[25] has shown promising results in modulating this pathway. Our study focused on the effects of Trillin on COX-2 expression in DU145 and PC3 cancer cell lines. Through western blot and RT-qPCR techniques, we observed a significant reduction in COX-2 protein and mRNA levels upon Trillin treatment (Figures 6A and 6B). Notably, this inhibition was dose-dependent, underscoring the potential of Trillin as a targeted therapeutic agent in COX-2 driven cancers.

In addition to its effect on COX-2, our study extended to examine Trillin's influence on the NF-κB pathway, a pivotal transcription factor in inflammation and regulator of COX-2 gene expression. We discovered that Trillin notably reduced the expression of phosphorylated IKKα/β (*p*-IKKα/β) and phosphorylated IκBα (*p*-IκBα), while had no effects on the levels of non-phosphorylated IKKα, IKKβ, and IκBα, demonstrating a dose-dependent inhibition on NF-κB pathway (Figure 6C). These findings suggest that Trillin's anti-inflammatory properties extend beyond COX-2 suppression, implicating it as a potential modulator of the NF-κB signaling pathway. Moreover, the dual-luciferase assay in 293T cells showed Trillin's dose-dependent suppression of NF-κB expression (Figure 6D). The specificity of Trillin's action on phosphorylated intermediates of this pathway underscores its therapeutic potential in diseases where NF-κB plays a key role. These findings not only highlight the versatility of Trillin but also pave the way for future investigations into its potential in cancer therapy.

Trillin modulates translocation of NF-κB p65/p50 into the nucleus, suppressing COX-2 transcriptional activation in CRPC cells

Next step of our study examined Trillin's ability to suppress COX-2 gene expression, which is regulated by transcription factors including NF-κB, using a streptavidin-agarose pull-down assay with a biotin-labeled COX-2 gene probe to demonstrate that Trillin significantly reduced dose-dependent binding of NF-κB p50 and p65 subunits to the COX-2 promoter (Figure 7A). Furthermore, analysis of whole-cell and nuclear lysates revealed a marked decrease in nuclear NF-κB p50 and p65 levels with Trillin treatment (Figure 7B). The integrity of the cytoplasmic and nuclear fractions was confirmed by detecting lamin B1 and beta-actin, showing minimal cross-contamination. These results indicate that Trillin effectively hinders the movement of NF-κB p50 and p65 from the cytoplasm into the nucleus, thereby impacting the regulation of COX-2 gene expression.

To validate our hypothesis regarding the impact of Trillin on NF-κB translocation, we employed an IFI assay in DU145 cells. The NF-κB p65 subunit was marked with red fluorescence, the p50 subunit with green fluorescence, and nuclear staining was performed using DAPI (blue). Figure 7C showed that in untreated controls, both p65 (red) and p50 (green) were predominantly located in the nucleus. However, Trillin treatment (10 μM or 20 μM for 48 h) led to the diffusion of these fluorescence markers out of the nucleus. These observations strongly indicate that Trillin inhibits translocation of NF-κB p65/p50 into the nucleus. Consequently, this substantiates the hypothesis that Trillin may hinder COX-2 transcriptional activation by modulating the nuclear localization of NF-κB subunits.

Trillin enhances miR-145-5p expression in CRPC cells, unveiling MAP3K11 as a target protein

Given the crucial role of miRNAs in the occurrence and development of PCa, we hypothesized that Trillin's anti-tumor effects might be mediated through miRNAs. We analyzed the GEO database (GSE21036)[24] and previous research works,[35,36] finding found that miR-145-5p exhibited significantly reduced expression specifically in castration-resistant prostate cancer (CRPC)

Figure 2. Trillin suppresses colony formation and disrupts the cell cycle in CRPC cells

(A) A clear reduction in colony formation in DU145 and PC3 cells following a 48-h Trillin treatment.

(B) Trillin treatment leads to an increase in cells in the G0/G1 phase and a decrease in the G2/M phase of cell cycle in both DU145 and PC3 cells.

(C) The levels of G1 phase cell cycle-related proteins CDK4 and cyclin D1 were evaluated in both cell lines using western blot. (Data were statistically analyzed with one way ANOVA and value was shown as mean ± SD of 3 independent experiments; $^{*}p < 0.05$; $^{**}p < 0.01$; $^{***}p < 0.001$).

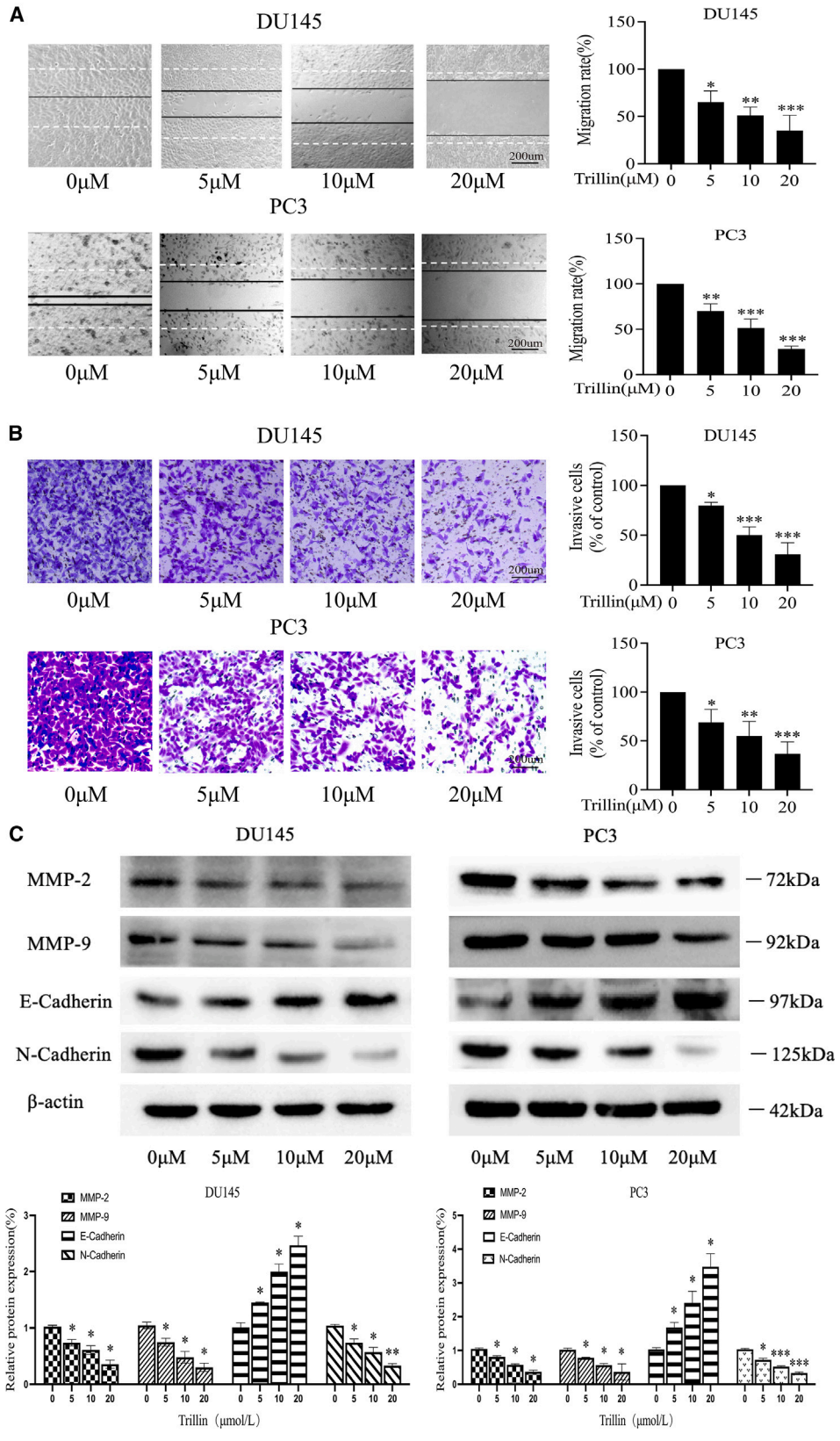

(legend on next page)

tissues and CRPC cell lines such as DU145, PC3, 22RV-1, or LNCap (Figure 8A). Subsequently, we assessed the effects of Trillin on miR-145-5p.

In CRPC cell lines DU145 and PC3, treatment with Trillin led to a dose-dependent increase in miR-145-5p mRNA levels (Figure 8B). Bioinformatics analysis revealed that miR-145-5p targets genes in the MAP kinase and transforming growth factor β (TGF-β) signaling pathways, specifically MAP3K3, MAP3K11, SMAD3, and TGFBR2 (Figure 8C). Analysis of StarBase database indicated that among these, only MAP3K11 is overexpressed in prostate cancer tissues (Figure 8D). Its expression correlates with the Gleason score and is highest in metastatic castration-resistant prostate cancer. The interaction between miR-145-5p and MAP3K11 was investigated using the TargetScan tool (Figure 8E) and validated through a dual-luciferase assay in 293T cells. Cells transfected with MAP3K11 wild type (WT) and miR-145-5p mimics showed reduced luciferase activity, whereas the MAP3K11 mutant type (MUT) plasmid did not affect the activity, confirming miR-145-5p's regulatory effect on MAP3K11 expression (Figure 8F).

Trillin downregulates MAP3K11 and inhibits inflammatory pathway molecules COX-2 and NF-κB via miR-145-5p in CRPC cells

In the study, DU145 and PC-3 cells underwent transfection with miR-145-5p mimics and inhibitors to analyze the impact on MAP3K11 mRNA using RT-qPCR. The results showed that miR-145-5p mimics reduced MAP3K11 mRNA levels in both cell lines (Figure 9A), whereas its inhibitor increased them, compared to their respective controls. This pattern was echoed in MAP3K11 protein levels as confirmed by western blot (Figure 9B), indicating miR-145-5p's negative regulation of MAP3K11's 3′UTR. Additionally, western blot experiments assessed the impact of miR-145-5p overexpression and MAP3K11 knockdown on COX-2/NF-κB pathway proteins. Both miR-145-5p overexpression and MAP3K11 knockdown reduced levels of *p*-IκBα, *p*-IKKβ, and COX-2 proteins, with their combined manipulation leading to a synergistic downregulation of these proteins, suggesting a potent regulatory effect on this pathway (Figure 10A). Western blot analysis assessed a significant decrease in MAP3K11 protein levels after Trillin treatment of CRPC cells, which was restored when miR-145-5p knockdown was combined with Trillin (Figure 10B).

Trillin suppresses the growth of CRPC xenografts in mice

To further elucidate Trillin's therapeutic potential, we extended an *in vivo* assessment, using immunodeficient NYG mice with induced tumors (Figure 11A). After treatment of Trillin, there was no significant change in mice body weight, indicating that Trillin did not have a notable toxic effect on the mice (Figure 11B). However, after 15 days of treatment with different concentrations of Trillin, there was a notable shrinkage observed in the tumor specimens (Figure 11C). Mice treated with Trillin at doses of 10 and 20 mg/kg/day for a duration of 15 days exhibited significant reductions in tumor size and weight, as compared to the control group (Figures 11D and 11E).

To investigate the molecular mechanisms underlying Trillin's anti-tumor effects, western blot analysis on the tumor tissues revealed that Trillin treatment led to a marked decrease in the expression of COX-2 and MAP3K11 proteins (Figure 11F) and immunohistochemical staining showed similar results (Figure 11G), which are known to play crucial roles in cancer progression. Furthermore, Trillin significantly increased the expression of miR-145-5p in the tumor tissues (Figure 11H), a microRNA known for its tumor-suppressive properties across various cancers.

The combined *in vitro* and *in vivo* findings suggest that Trillin exerts its anti-cancer effects in prostate cancer through multiple pathways. By elevating miR-145-5p levels, Trillin suppresses MAP3K11 expression, which is integral to the NF-κB/COX-2 signaling pathway. This pathway is known for its role in tumor progression and resistance to therapy. Additionally, Trillin's ability to induce apoptosis, halt cell cycle progression, and impede cell invasion and metastasis further underscores its potential as a therapeutic agent against CRPC, a particularly aggressive form of the prostate cancer. These multifaceted anti-cancer actions position Trillin as a promising candidate for further development and clinical investigation in the context of prostate cancer treatment.

DISCUSSION

Globally, PCa is a predominant male malignant tumor, with its morbidity and mortality escalating due to population aging and environmental lifestyle changes.[37] Despite the availability of treatment such as surgery, radiotherapy, chemotherapy, and androgen deprivation therapy, PCa often progresses to CRPC, a stage characterized by limited treatment options and high side effects. Given the urgent need for effective and safe treatments for CRPC, studies have emphasized the importance of traditional Chinese medicine in enhancing clinical outcomes and postoperative survival rates of prostate cancer patients.[38] Our study specifically examines the effect of Trillin on CRPC cell proliferation and metastatic ability, and its underlying mechanisms, proposing an effective adjuvant therapy for CRPC treatment.

In the present study, we had identified that Trillin exerted its anticancer activity through the upregulation of miR-145-5p, which in turn targets MAP3K11, a key upstream regulator in the

Figure 3. Effect of Trillin on CRPC cells migration and invasion

(A) A scratch assay demonstrates the diminished migration rates of DU145 and PC3 cells following 48-h Trillin exposure at specified concentrations (original magnification, 100×). Scale bar: 200 μm.

(B) Invasion analysis demonstrates the inhibitory impact of Trillin on cell invasion, with quantification of cells that successfully crossed the Matrigel-lined Transwell chambers (original magnification, 200×). Scale bar: 100 μm.

(C) Western blot analysis was employed to evaluate the expression of invasive marker proteins in both cell lines. (Data were statistically analyzed with one way ANOVA and value was shown as mean ± SD of 3 independent experiments; $^{*}p < 0.05$; $^{**}p < 0.01$; $^{***}p < 0.001$).

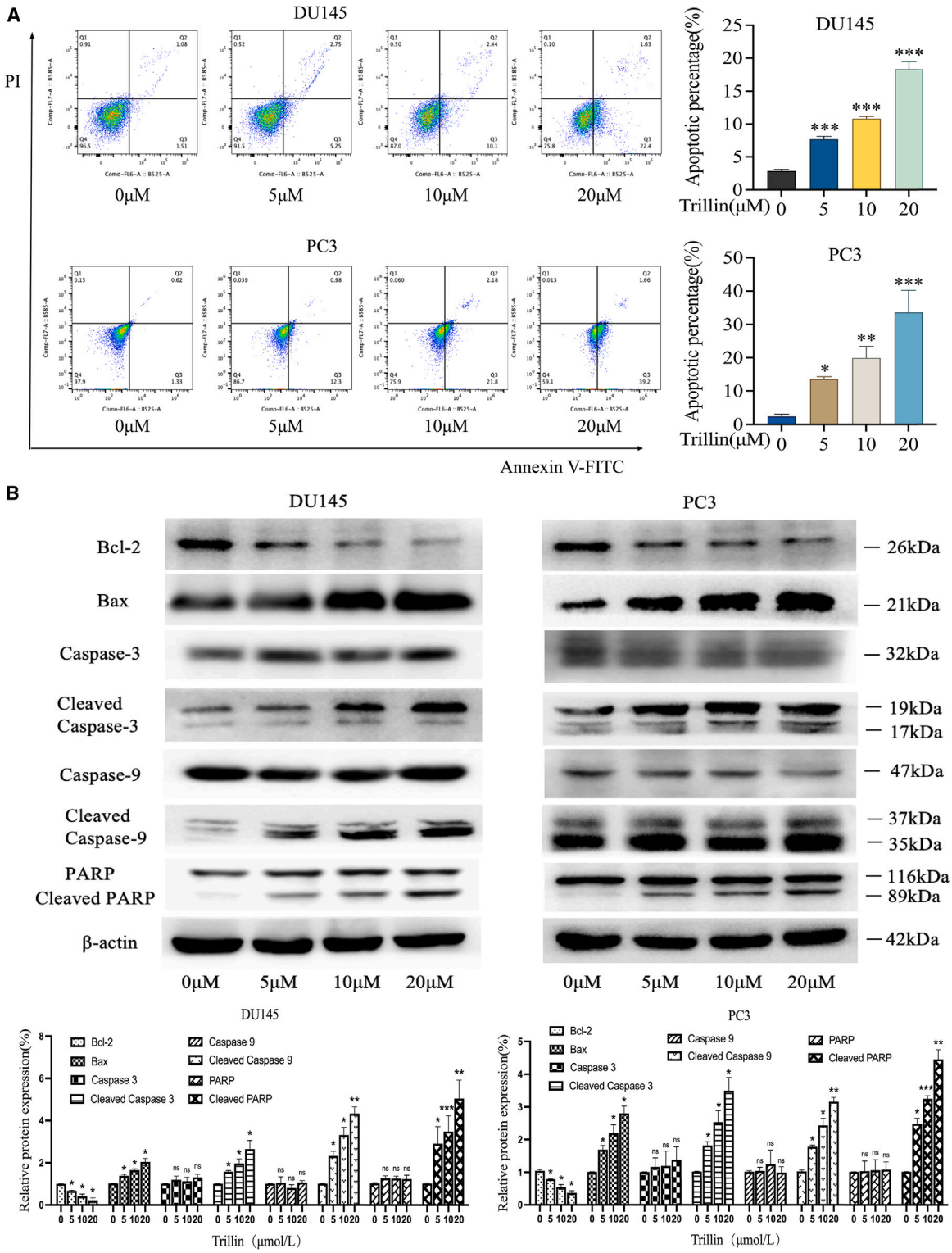

Figure 4. Trillin induces apoptosis in CRPC cells via caspase pathway modulation

(A) Apoptosis levels were measured using a CytoFLEX flow cytometer following a 48-h treatment, with the percentage of apoptotic cells subsequently calculated. (B) The protein expressions of Bcl-2, Bax, caspase-3, cleaved caspase-3, caspase-9, cleaved caspase-9, PARP and cleaved PARP in DU145 and PC3 cells were quantified through western blot analysis. (Data were statistically analyzed with one way ANOVA and value was shown as mean ± SD of 3 independent experiments; ns indicates not significant; $^{*}p < 0.05$; $^{**}p < 0.01$; $^{***}p < 0.001$).

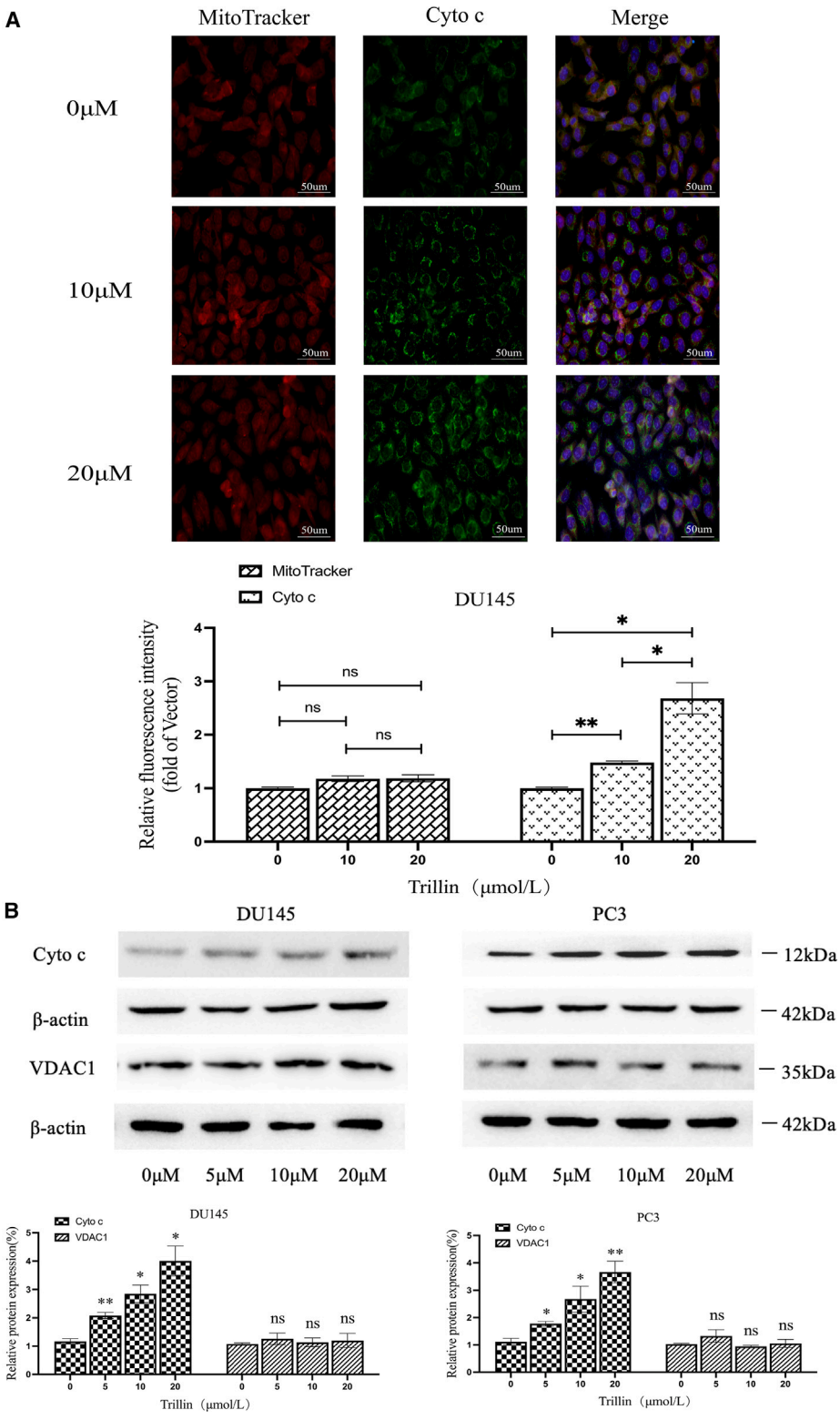

Figure 5. Trillin induces apoptosis in CRPC cells by increasing the release of cyto *c* from mitochondria

(A) Cyto *c* release from mitochondria to the cytoplasm in DU145 cells was observed using immunofluorescence analysis. Scale bar: 50 μm.

(B) Cyto *c* and VDAC1 protein levels in both cell types were evaluated via western blot. (Data were statistically analyzed with one way ANOVA and value was shown as mean ± SD of 3 independent experiments; ns indicates not significant; *$p < 0.05$; **$p < 0.01$; ***$p < 0.001$).

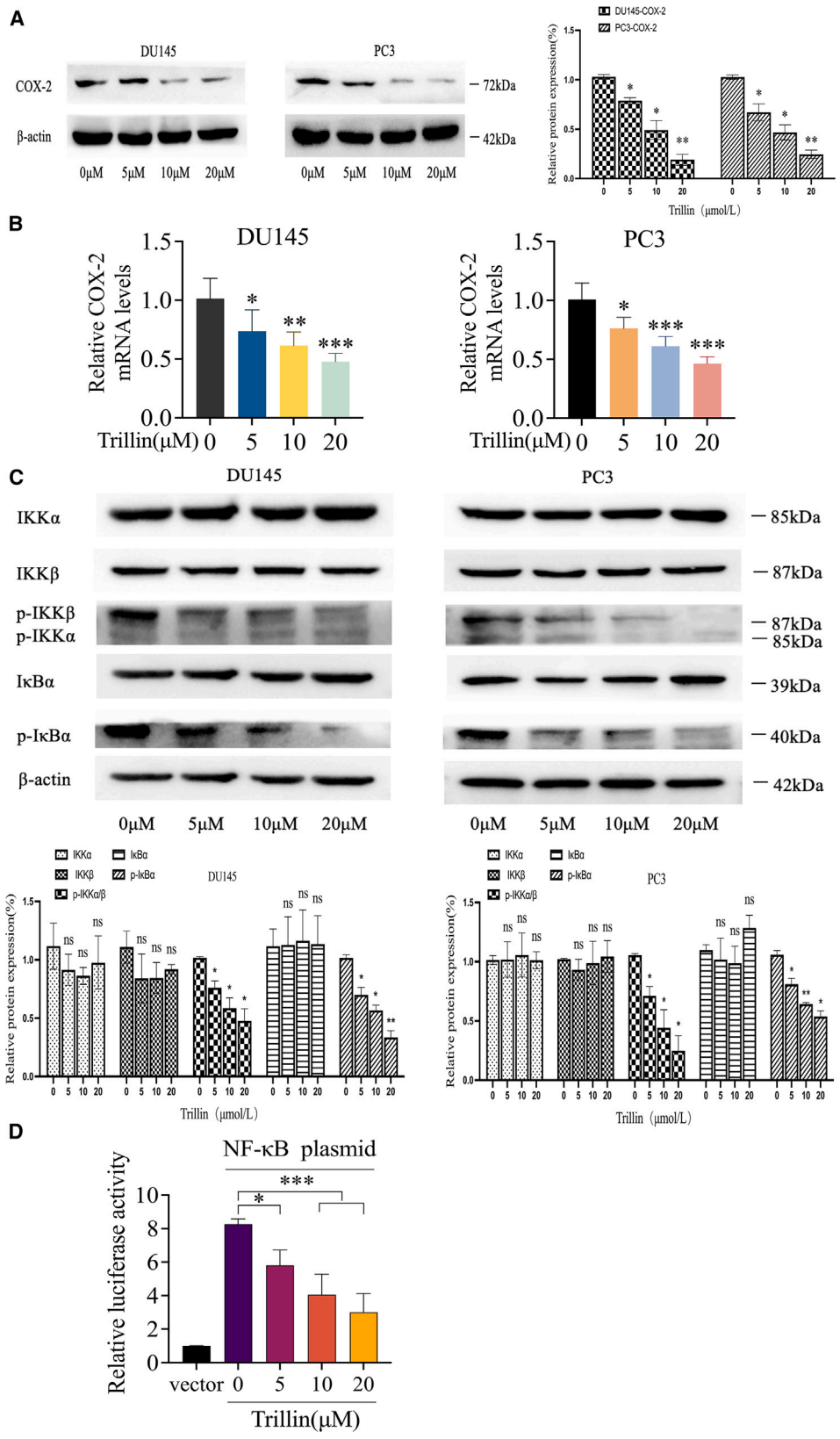

(legend on next page)

MAPK signaling pathway. The overexpression of miR-145-5p leads to the downregulation of MAP3K11, thereby attenuating the downstream signaling events in the NF-κB and COX-2 pathways. Specifically, we observed the following. (1) miR-145-5p upregulation: Trillin treatment significantly increased the levels of miR-145-5p in CRPC cell lines. (2) MAP3K11 downregulation: the upregulation of miR-145-5p resulted in the suppression of MAP3K11, which is known to activate the NF-κB and MAPK pathways. (3) NF-κB/COX-2 pathway inhibition: with the downregulation of MAP3K11, there was a subsequent decrease in the phosphorylation and activation of IKKα/β and IκBα, leading to reduced nuclear translocation of NF-κB subunits (p50 and p65). This inhibition was further confirmed by decreased COX-2 expression at both mRNA and protein levels. Furthermore, Trillin primarily regulates these signaling proteins indirectly through the upregulation of miR-145-5p, which targets the 3′UTR of MAP3K11 mRNA, leading to its degradation and reduced translation. The suppression of MAP3K11 subsequently impacts the NF-κB and COX-2 signaling pathways, which are crucial for the inflammatory and proliferative responses in CRPC cells.

In addition, we have performed dual-luciferase reporter assays and western blot analyses to validate the interaction between miR-145-5p and MAP3K11, and to measure the downstream effects on NF-κB and COX-2. These results confirm that Trillin's anticancer effects are mediated through this indirect pathway, highlighting the crucial role of miR-145-5p in regulating these oncogenic signals. miR-145-5p has garnered attention for its inhibitory effects on the proliferation and progression of various cancers, including colorectal cancer,[39] breast cancer[40] and bladder cancer.[41] Additionally, it also plays a crucial role in prostate cancer by impeding bone metastasis[42] and restraining neuroendocrine differentiation.[36] However, there is a scarcity of research on therapeutic drugs targeting miR-145-5p in cancer studies, especially for CRPC. In this study, we conducted an investigation into the correlation between the anti-cancer effects of Trillin and the expression of miR-145-5p. We observed a significant elevation in miR-145-5p levels post-Trillin treatment, a finding corroborated in Trillin-treated mouse PCa xenograft tumors. Intriguingly, the expression of miR-145-5p in CRPC cells showed a dose-responsive increase to Trillin exposure. These findings propose miR-145-5p as a potential molecular mediator of Trillin's therapeutic efficacy against prostate cancer.

The activation of the NF-κB and MAPK pathways significantly influences the tumor's biological behavior of prostate cancer,[43,44] as they respond to extracellular stimuli, such as cytokines, growth factors, and stress signals, that is frequently triggered by the tumor microenvironment in prostate cancer, leading to the development and progression.[45,46]

Therefore, repression of the activation of these pathways emerges as a potentially efficacious therapeutic strategy for prostate cancer. MiRNAs, particularly miR-145-5p, are known to modulate gene expression by binding to the 3′UTR of target mRNAs, leading to mRNA degradation or translation inhibition.[47] Previous research has shown that miR-145-5p downregulates the NF-κB pathway.[48] However, the precise mechanism remains unclear. Our results provide further evidence that miR-145-5p suppresses the activation of the NF-κB pathway, reflecting in reduced levels of *p*-IκBα, *p*-IKKβ, and inflammatory mediator COX-2, and a decrease in the nuclear translocation of p50/p65. Moreover, MAP3K11, one member of the MAPK family, exhibits the highest levels in mCRPC cases and is associated with the progress of prostate cancer. In the present study, MAP3K11 was identified as a downstream target of miR-145-5p. Trillin could induce the expression of miR-145-5p and reduced the expression of MAP3K11. These findings suggest that Trillin may exert its inhibitory effects on the NF-κB and MAP3K11 pathways via miR-145-5p.

Limitations of the study

The use of *in vitro* cell lines may not fully reflect the complexities of the tumor microenvironment. The concentration range of Trillin tested may not capture its complete pharmacological profile, and the short incubation periods might overlook long-term effects. Focusing solely on Trillin without considering combination therapies limits the findings, and while multiple cell lines were used, they may not represent the full diversity of castration-resistant prostate cancer. Future research should address these limitations to better validate Trillin's therapeutic potential.

RESOURCE AVAILABILITY

Lead contact

Further information and requests for resources and reagents should be directed to and will be fulfilled by the lead contact, Zhiyu Liu (Z.L.), (zyliu@dmu.edu.cn.).

Materials availability

This study did not generate new unique reagents and all materials in this study are commercially available.

Data and code availability

- All the data reported in this study will be shared by the lead contact upon request. This paper analyzes existing, publicly available data. These accession numbers for the datasets are listed in the key resources table.
- This study does not report any original code.
- Any additional information required to reanalyze the data reported in this paper is available from the lead contact upon request.

ACKNOWLEDGMENTS

We thank all those who participated in this study. This work was supported by The Scientific Research Project of Ministry of Education of Liaoning Province (LJKZZ20220100), The Interdisciplinary Research Cooperation Project Team

Figure 6. Trillin's impact on COX-2 and NF-κB expression in CRPC cells

DU145 and PC3 cells were treated with Trillin at the indicated doses after 48 h.

(A) Western blot was employed to analyze COX-2 protein expression levels.

(B) The gene expression was assessed using qRT-PCR analyses.

(C) Western blot was used to measure the levels of *p*-IKKα/β, IKKα, IKKβ, *p*-IκBα, and IκBα proteins.

(D) The dual-luciferase assay in 293T cells showed Trillin's dose-dependent suppression of NF-κB expression. (Data were statistically analyzed with one way ANOVA and value was shown as mean ± SD of 3 independent experiments; ns indicates not significant; $^{*}p < 0.05$; $^{**}p < 0.01$; $^{***}p < 0.001$).

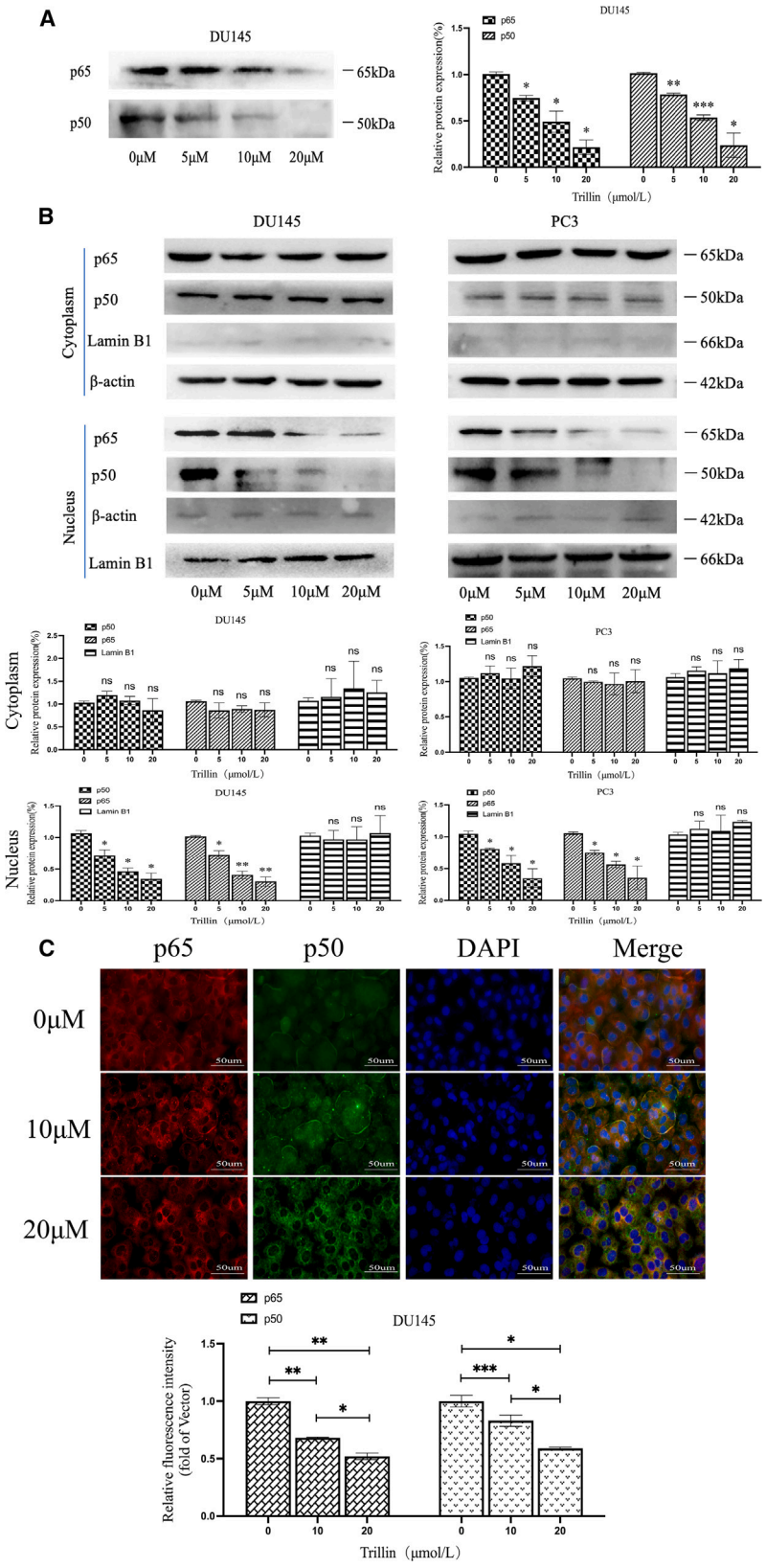

Figure 7. Trillin effectively inhibits both the translocation of NF-κB p50 and p65 to the nucleus and their binding to the COX-2 promoter

(A) In DU145 cells treated with Trillin for 48 h, the binding of p50 and p65 to the COX-2 promoter was evaluated using pulldown assays.

(B) The study used western blot to assess p50 and p65 protein levels, separating cytoplasmic and nuclear proteins with lamin B1 and β-actin as respective loading controls.

(C) Additionally, confocal microscopy was performed to observe the subcellular distribution of p50 and p65 at 48 h post-treatment. Scale bar: 50 μm. (Data were statistically analyzed with one way ANOVA and value was shown as mean ± SD of 3 independent experiments; ns indicates not significant; $^{*}p < 0.05$; $^{**}p < 0.01$; $^{***}p < 0.001$).

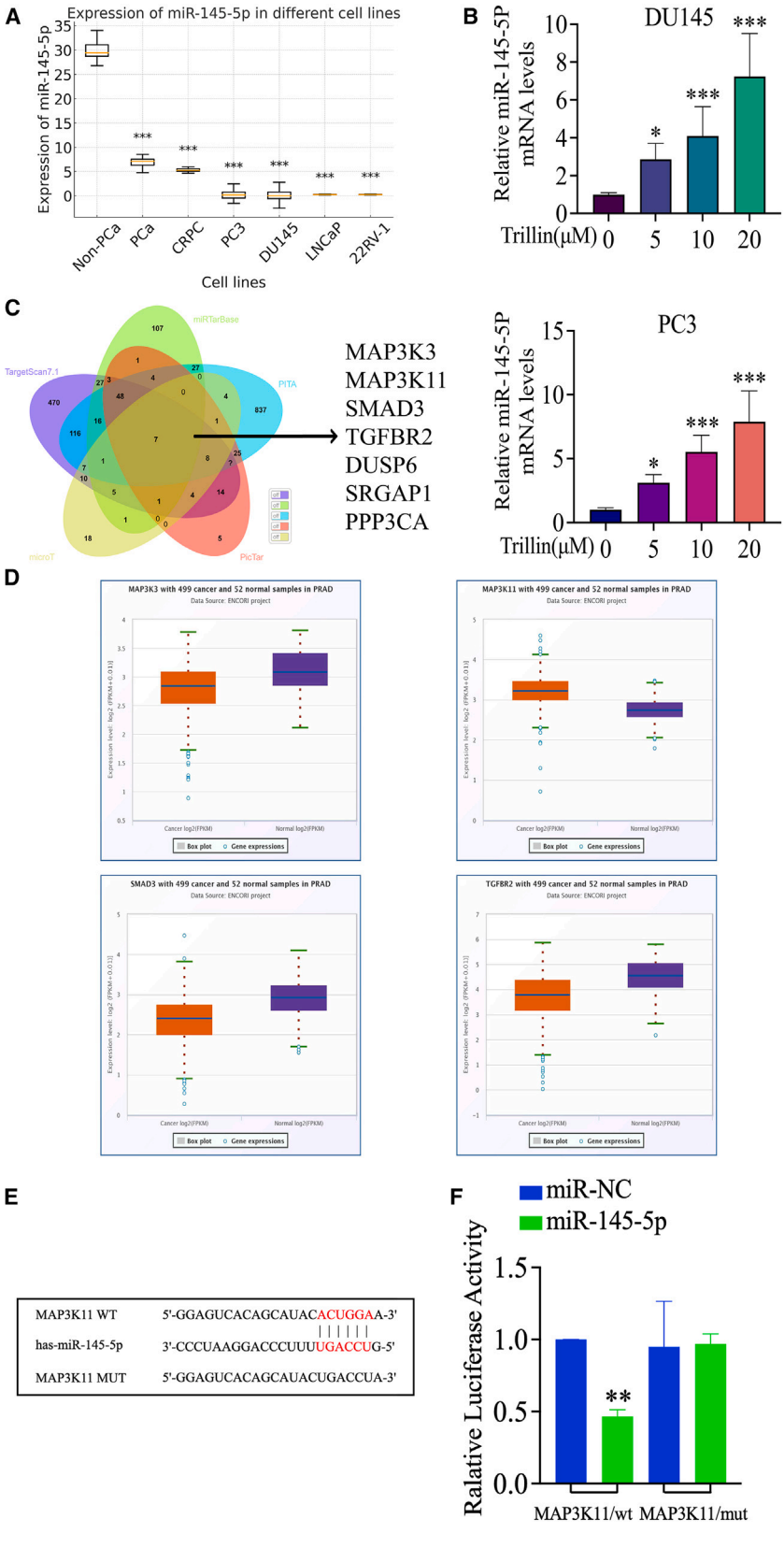

Figure 8. Trillin promotes the expression of miR-145-5p in CRPC cells and exerts its effects through binding with MAP3K11

(A) miR-145-5p serves as a tumor-suppressive molecule and is downregulated in prostate cancer, especially in CRPC patients and CRPC cell lines DU145 or PC3 (n: numbers of patients).

(B) qRT-PCR of DU145 and PC3 cells treated with Trillin for 48 h showed an increase in miR-145-5p in a dose-dependent manner.

(C) Bioinformatics analysis predicts downstream targets of miR-145-5p.

(D) Expression analysis of miR-145-5p target inflammation molecules in prostate cancer and normal tissues using TCGA data.

(E) The TargetScan website predicts binding sites of miR-145-5p and MAP3K11.

(F) A dual-luciferase assay validates the binding of miR-145-5p to MAP3K11 in 293T cells. (Data were statistically analyzed with one way ANOVA and value was shown as mean ± SD of 3 independent experiments; $^{*}p < 0.05$; $^{**}p < 0.01$; $^{***}p < 0.001$).

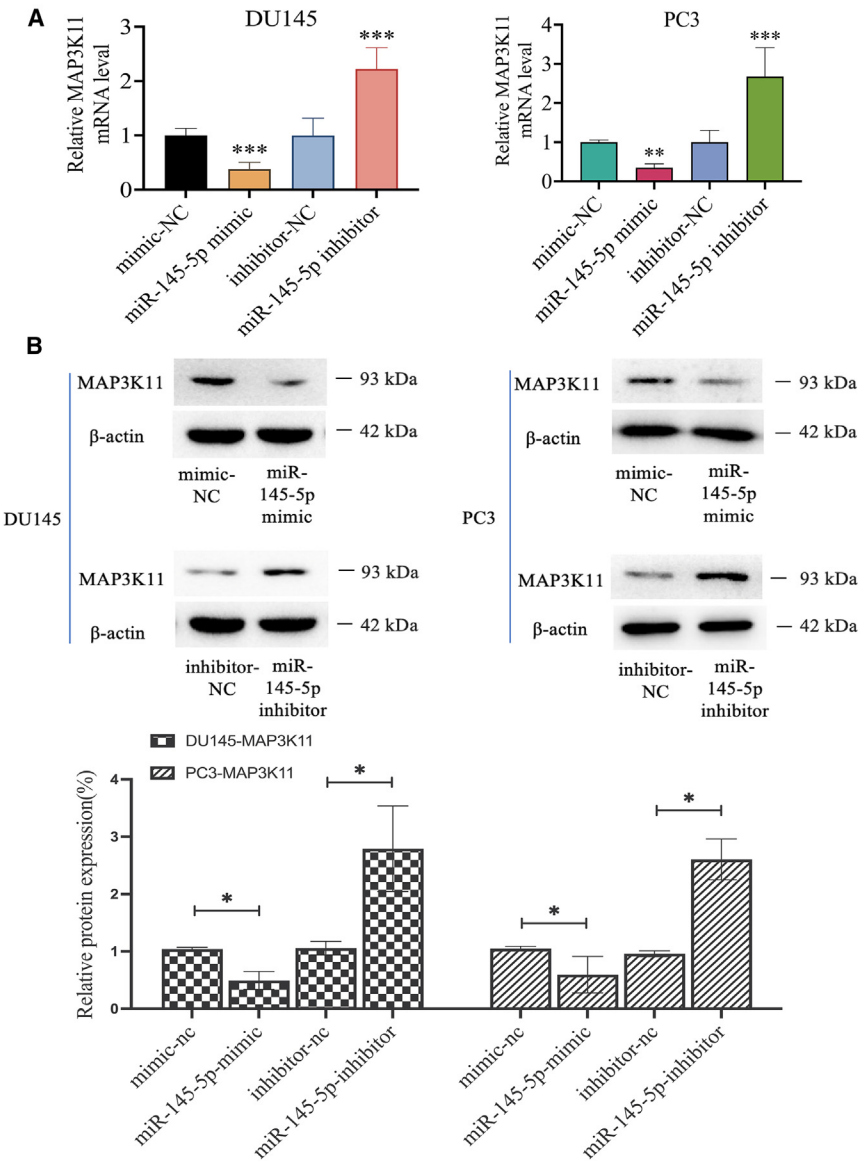

Figure 9. miR-145-5p directly downregulates MAP3K11 expression in CRPC

(A) RT-qPCR analysis of MAP3K11 in DU145 and PC3 cells following transfection with miR-145-5p mimic, inhibitor, or negative control (NC).

(B) Western blot analysis of MAP3K11 protein levels in DU145 and PC3 cells in response to miR-145-5p overexpression or knockdown. (Data were statistically analyzed with one way ANOVA and value was shown as mean ± SD of 3 independent experiments; $^{*}p < 0.05$; $^{**}p < 0.01$; $^{***}p < 0.001$).

Funding of Dalian Medical University Planning and research category (focusing on planning for recreation) (JCHZ2023001), and The United Foundation for Dalian Institute of Chemical Physics, Chinese Academy of Sciences and the Second Hospital of Dalian Medical University (DMU-2 & DICP UN202304).

AUTHOR CONTRIBUTIONS

Z.Y. conceived the idea of the study. Yanlong Wang, Y.P., W.H., and C.H. performed the experiments. Yanlong Wang analyzed and interpreted the data, created figures, and wrote the text. X.G. and P.L. developed the statistical analysis plan and conducted statistical analyses. L.W. and Z.L. helped to design experiments. H.Z. and W.H. conducted bioinformation analyses. Ying Wang drafted the original manuscript. All authors reviewed the manuscript draft and revised it critically on intellectual content. All authors approved the final version of the manuscript to be published.

DECLARATION OF INTERESTS

The authors declare no competing interests.

STAR★METHODS

Detailed methods are provided in the online version of this paper and include the following:

- KEY RESOURCES TABLE
- EXPERIMENTAL MODEL AND STUDY PARTICIPANT DETAILS
  - Cell culture
  - Animal experiments
- METHOD DETAILS
  - Cell viability assay
  - Colony formation assay
  - Wound healing assay
  - Transwell invasion assay
  - Flow cytometry
  - Confocal immunofluorescence analysis
  - Western blot
  - qRT-PCR
  - Cell transfection

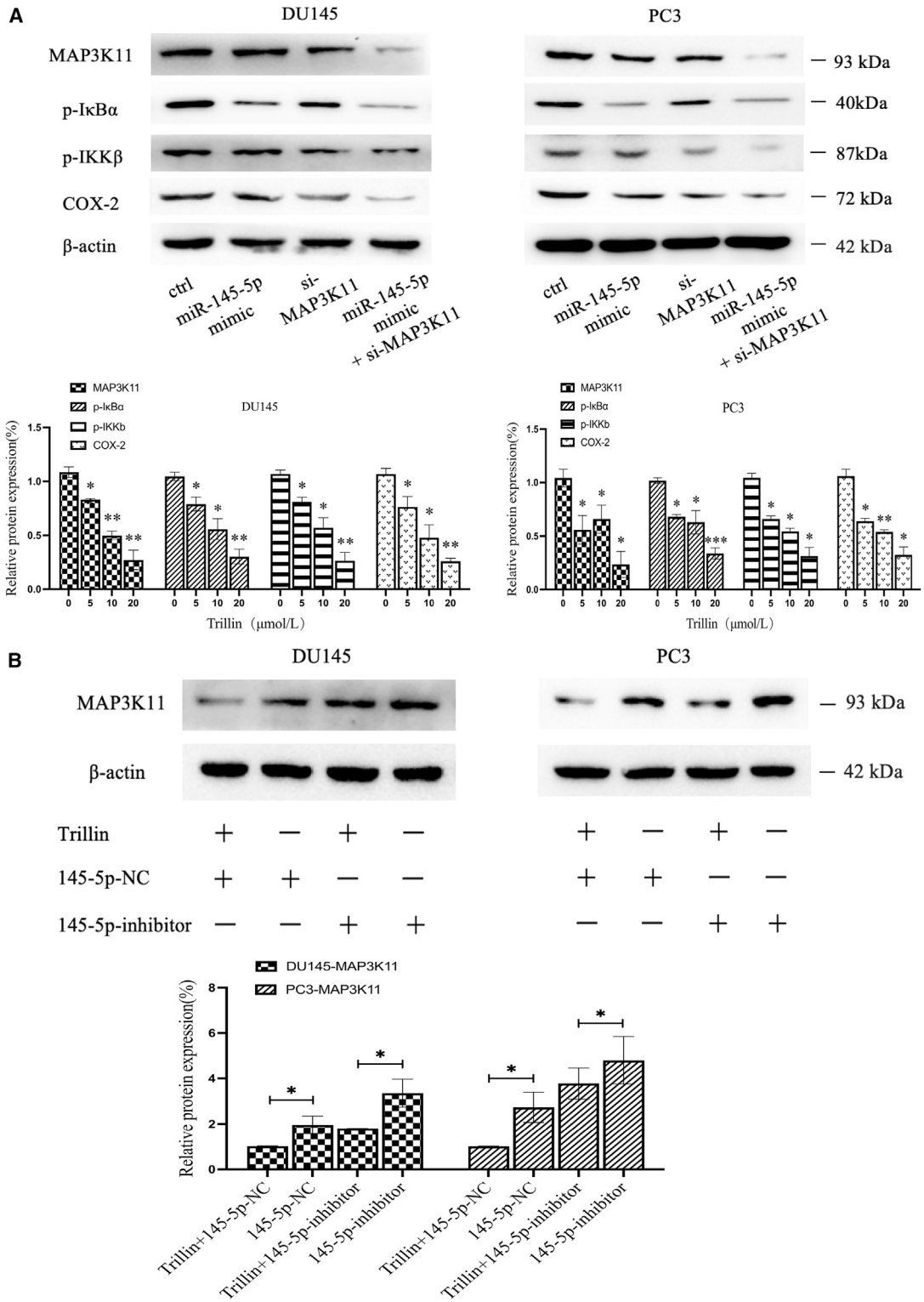

Figure 10. Trillin upregulates miR-145-5p, thereby inhibiting MAP3K11, leading to the suppression of downstream NF-κB/COX-2 signaling

(A) Western blot analysis to show the individual and combined impacts of miR-145-5p overexpression and MAP3K11 knockdown on MAP3K11, *p*-IκBα, *p*-IKKβ, and COX-2 protein levels in the pathway.

(B) Western blot analysis assessed the effect of Trillin treatment, miR-145-5p knockdown, or a combination of both on MAP3K11 protein levels in DU145 and PC3 cells. (Data were statistically analyzed with one way ANOVA and value was shown as mean ± SD of 3 independent experiments; $^{*}p < 0.05$; $^{**}p < 0.01$; $^{***}p < 0.001$).

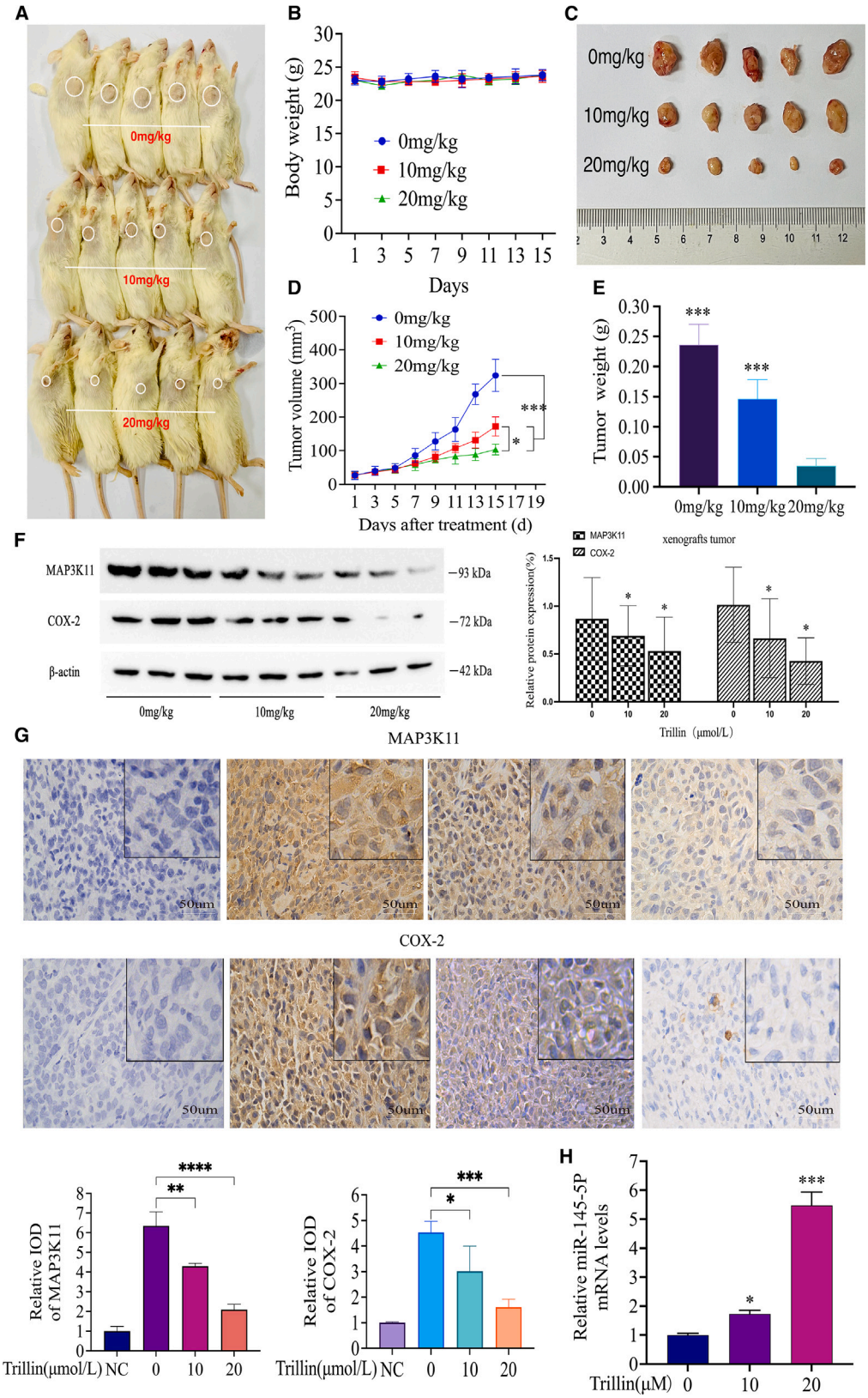

(legend on next page)

- Streptavidin-agarose pulldown assay
- Dual-luciferase assay
- Bioinformatics analysis of public database reanalysis

- QUANTIFICATION AND STATISTICAL ANALYSIS

Received: April 10, 2024
Revised: July 4, 2024
Accepted: November 27, 2024
Published: December 2, 2024

REFERENCES

1. Siegel, R.L., Miller, K.D., Wagle, N.S., and Jemal, A. (2023). Cancer statistics, 2023. CA. Cancer J. Clin. *73*, 17–48.
2. Wang, F., Wang, C., Xia, H., Lin, Y., Zhang, D., Yin, P., and Yao, S. (2022). Burden of Prostate Cancer in China, 1990-2019: Findings From the 2019 Global Burden of Disease Study. Front. Endocrinol. *13*, 853623.
3. Gillessen, S., Bossi, A., Davis, I.D., de Bono, J., Fizazi, K., James, N.D., Mottet, N., Shore, N., Small, E., Smith, M., et al. (2023). Management of Patients with Advanced Prostate Cancer. Part I: Intermediate-/High-risk and Locally Advanced Disease, Biochemical Relapse, and Side Effects of Hormonal Treatment: Report of the Advanced Prostate Cancer Consensus Conference 2022. Eur. Urol. *83*, 267–293.
4. Hatano, K., and Nonomura, N. (2023). Systemic Therapies for Metastatic Castration-Resistant Prostate Cancer: An Updated Review. World J. Mens Health *41*, 769–784.
5. Sánchez, B.G., Bort, A., Mateos-Gómez, P.A., Rodríguez-Henche, N., and Díaz-Laviada, I. (2019). Combination of the natural product capsaicin and docetaxel synergistically kills human prostate cancer cells through the metabolic regulator AMP-activated kinase. Cancer Cell Int. *19*, 54.
6. Zheng, X., Jiang, Z., Li, X., Zhang, C., Li, Z., Wu, Y., Wang, X., Zhang, C., Luo, H.B., Xu, J., and Wu, D. (2018). Screening, synthesis, crystal structure, and molecular basis of 6-amino-4-phenyl-1,4-dihydropyrano[2,3-c] pyrazole-5-carbonitriles as novel AKR1C3 inhibitors. Bioorg. Med. Chem. *26*, 5934–5943.
7. Prelaj, A., Rebuzzi, S.E., Buzzacchino, F., Pozzi, C., Ferrara, C., Frantellizzi, V., Follacchio, G.A., Civitelli, L., De Vincentis, G., Tomao, S., and Bianco, V. (2019). Radium-223 in patients with metastatic castration-resistant prostate cancer: Efficacy and safety in clinical practice. Oncol. Lett. *17*, 1467–1476.
8. Cai, J., Zhao, J., Gao, P., and Xia, Y. (2022). Patchouli alcohol suppresses castration-resistant prostate cancer progression by inhibiting NF-κB signal pathways. Transl. Androl. Urol. *11*, 528–542.
9. Hanahan, D. (2022). Hallmarks of Cancer: New Dimensions. Cancer Discov. *12*, 31–46.
10. Zhou, M., Liang, J., Hui, J., and Xu, J. (2023). Inflammation-related indicators have a potential to increase overall quality of the prostate cancer management: a narrative review. Transl. Androl. Urol. *12*, 809–822.
11. Guo, C., Sharp, A., Gurel, B., Crespo, M., Figueiredo, I., Jain, S., Vogl, U., Rekowski, J., Rouhifard, M., Gallagher, L., et al. (2023). Targeting myeloid chemotaxis to reverse prostate cancer therapy resistance. Nature *623*, 1053–1061.
12. Thomas-Jardin, S.E., Dahl, H., Nawas, A.F., Bautista, M., and Delk, N.A. (2020). NF-κB signaling promotes castration-resistant prostate cancer initiation and progression. Pharmacol. Ther. *211*, 107538.
13. Guo, W., Zhang, Z., Li, G., Lai, X., Gu, R., Xu, W., Chen, H., Xing, Z., Chen, L., Qian, J., et al. (2020). Pyruvate Kinase M2 Promotes Prostate Cancer Metastasis Through Regulating ERK1/2-COX-2 Signaling. Front. Oncol. *10*, 544288.
14. Krawczyk, M., and Emerson, B.M. (2014). p50-associated COX-2 extragenic RNA (PACER) activates COX-2 gene expression by occluding repressive NF-κB complexes. Elife *3*, e01776.
15. Li, J., Liu, N., Zhou, H., Xian, P., Song, Y., Tang, X., Li, Y., and Basler, M. (2023). Immunoproteasome inhibition prevents progression of castration-resistant prostate cancer. Br. J. Cancer *128*, 1377–1390.
16. Gavrikova, T., Nakamura, N., Davydova, J., Antonarakis, E.S., and Yamamoto, M. (2023). Infectivity-Enhanced, Conditionally Replicative Adenovirus for COX-2-Expressing Castration-Resistant Prostate Cancer. Viruses *15*, 901.
17. Baltimore, D., Boldin, M.P., O'Connell, R.M., Rao, D.S., and Taganov, K.D. (2008). MicroRNAs: new regulators of immune cell development and function. Nat. Immunol. *9*, 839–845.
18. Xu, W.X., Liu, Z., Deng, F., Wang, D.D., Li, X.W., Tian, T., Zhang, J., and Tang, J.H. (2019). MiR-145: a potential biomarker of cancer migration and invasion. Am. J. Transl. Res. *11*, 6739–6753.
19. Xu, W., Hua, Y., Deng, F., Wang, D., Wu, Y., Zhang, W., and Tang, J. (2020). MiR-145 in cancer therapy resistance and sensitivity: A comprehensive review. Cancer Sci. *111*, 3122–3131.
20. Coradduzza, D., Cruciani, S., Arru, C., Garroni, G., Pashchenko, A., Jedea, M., Zappavigna, S., Caraglia, M., Amler, E., Carru, C., and Maioli, M. (2022). Role of miRNA-145, 148, and 185 and Stem Cells in Prostate Cancer. Int. J. Mol. Sci. *23*, 1626.
21. Gao, K., Li, X., Ni, J., Wu, B., Guo, J., Zhang, R., and Wu, G. (2023). Non-coding RNAs in enzalutamide resistance of castration-resistant prostate cancer. Cancer Lett. *566*, 216247.
22. Arrighetti, N., and Beretta, G.L. (2021). miRNAs as Therapeutic Tools and Biomarkers for Prostate Cancer. Pharmaceutics *13*, 380.
23. Chen, W., Yao, G., and Zhou, K. (2019). miR-103a-2-5p/miR-30c-1-3p inhibits the progression of prostate cancer resistance to androgen ablation therapy via targeting androgen receptor variant 7. J. Cell. Biochem. *120*, 14055–14064.
24. Goto, Y., Kurozumi, A., Arai, T., Nohata, N., Kojima, S., Okato, A., Kato, M., Yamazaki, K., Ishida, Y., Naya, Y., et al. (2017). Impact of novel miR-145-3p regulatory networks on survival in patients with castration-resistant prostate cancer. Br. J. Cancer *117*, 409–420.
25. Silva, J., Tavares, V., Afonso, A., Garcia, J., Cerqueira, F., and Medeiros, R. (2023). Plasmatic MicroRNAs and Treatment Outcomes of Patients with Metastatic Castration-Resistant Prostate Cancer: A Hospital-Based Cohort Study and In Silico Analysis. Int. J. Mol. Sci. *24*, 9101.
26. Zhu, J., Wang, S., Zhang, W., Qiu, J., Shan, Y., Yang, D., and Shen, B. (2015). Screening key microRNAs for castration-resistant prostate cancer based on miRNA/mRNA functional synergistic network. Oncotarget *6*, 43819–43830.

Figure 11. Trillin effectively inhibits the growth of CRPC xenografts in mice

(A) A subcutaneous tumor model was established in NYG mice through the transplantation of DU145 cells.
(B) Administering various concentrations of Trillin did not significantly affect the body weight of the mice.
(C) After 15 days of Trillin treatment, there was a notable reduction observed in the tumor specimen.
(D) The tumor volume noticeably decreased as Trillin's concentration increased.
(E) The tumor weight significantly decreased with increasing concentrations of Trillin.
(F) Western blot analysis was conducted to assess the protein expressions of MAP3K11 and COX-2 in tumor tissues.
(G) Immunohistochemical analysis was utilized to visualize the protein expression of MAP3K11 and COX-2 in tumor tissues (original magnification, 400×). Scale bar: 50 μm.
(H) RT-qPCR analysis was employed to measure the expression of miR-145-5p in tumor tissues. (Data were statistically analyzed with one way ANOVA and value was shown as mean ± SD of 3 independent experiments; $^{*}p < 0.05$; $^{**}p < 0.01$; $^{***}p < 0.001$).

27. Qian, S., Tong, S., Wu, J., Tian, L., Qi, Z., Chen, B., Zhu, D., and Zhang, Y. (2020). Paris saponin VII extracted from Trillium tschonoskii induces autophagy and apoptosis in NSCLC cells. J. Ethnopharmacol. *248*, 112304.
28. Zhan, G., Wei, T., Xie, H., Xie, X., Hu, J., Tang, H., Cheng, Y., Liu, H., Li, S., and Yang, G. (2023). Autophagy inhibition mediated by trillin promotes apoptosis in hepatocellular carcinoma cells via activation of mTOR/STAT3 signaling. Naunyn-Schmiedeberg's Arch. Pharmacol. *397*, 1575–1587.
29. Zhan, G., Hu, J., Xiao, B., Wang, X., Yang, Z., Yang, G., and Lu, L. (2020). Trillin prevents proliferation and induces apoptosis through inhibiting STAT3 nuclear translocation in hepatoma carcinoma cells. Med. Oncol. *37*, 44.
30. Liu, M.J., Wang, Z., Ju, Y., Zhou, J.B., Wang, Y., and Wong, R.N.S. (2004). The mitotic-arresting and apoptosis-inducing effects of diosgenyl saponins on human leukemia cell lines. Biol. Pharm. Bull. *27*, 1059–1065.
31. Rodríguez-Ubreva, F.J., Cariaga-Martinez, A.E., Cortés, M.A., Romero-De Pablos, M., Ropero, S., López-Ruiz, P., and Colás, B. (2010). Knockdown of protein tyrosine phosphatase SHP-1 inhibits G1/S progression in prostate cancer cells through the regulation of components of the cell-cycle machinery. Oncogene *29*, 345–355.
32. Yu, Z., Guo, W., Ma, X., Zhang, B., Dong, P., Huang, L., Wang, X., Wang, C., Huo, X., Yu, W., et al. (2023). Correction: Gamabufotalin, a bufadienolide compound from toad venom, suppresses COX-2 expression through targeting IKKβ/NF-κB signaling pathway in lung cancer cells. Mol. Cancer *22*, 144.
33. Ren, Q., Hou, Y., Li, X., and Fan, X. (2020). Silence of TPPP3 suppresses cell proliferation, invasion and migration via inactivating NF-κB/COX2 signal pathway in breast cancer cell. Cell Biochem. Funct. *38*, 773–781.
34. Tan, H., He, Q., Li, R., Lei, F., and Lei, X. (2016). Trillin Reduces Liver Chronic Inflammation and Fibrosis in Carbon Tetrachloride (CCl4) Induced Liver Injury in Mice. Immunol. Invest. *45*, 371–382.
35. Liu, J., Li, J., Ma, Y., Xu, C., Wang, Y., and He, Y. (2021). MicroRNA miR-145-5p inhibits Phospholipase D 5 (PLD5) to downregulate cell proliferation and metastasis to mitigate prostate cancer. Bioengineered *12*, 3240–3251.
36. Ji, S., Shi, Y., Yang, L., Zhang, F., Li, Y., and Xu, F. (2022). miR-145-5p Inhibits Neuroendocrine Differentiation and Tumor Growth by Regulating the SOX11/MYCN Axis in Prostate cancer. Front. Genet. *13*, 790621.
37. Xia, C., Dong, X., Li, H., Cao, M., Sun, D., He, S., Yang, F., Yan, X., Zhang, S., Li, N., and Chen, W. (2022). Cancer statistics in China and United States, 2022: profiles, trends, and determinants. Chin. Med. J. *135*, 584–590.
38. Wang, X., Fang, G., and Pang, Y. (2018). Chinese Medicines in the Treatment of Prostate Cancer: From Formulas to Extracts and Compounds. Nutrients *10*, 283.
39. Chen, Q., Zhou, L., Ye, X., Tao, M., and Wu, J. (2020). miR-145-5p suppresses proliferation, metastasis and EMT of colorectal cancer by targeting CDCA3. Pathol. Res. Pract. *216*, 152872.
40. Tang, W., Zhang, X., Tan, W., Gao, J., Pan, L., Ye, X., Chen, L., and Zheng, W. (2019). miR-145-5p Suppresses Breast Cancer Progression by Inhibiting SOX2. J. Surg. Res. *236*, 278–287.
41. Zhang, H., Jiang, M., Liu, Q., Han, Z., Zhao, Y., and Ji, S. (2018). miR-145-5p inhibits the proliferation and migration of bladder cancer cells by targeting TAGLN2. Oncol. Lett. *16*, 6355–6360.
42. Luo, B., Yuan, Y., Zhu, Y., Liang, S., Dong, R., Hou, J., Li, P., Xing, Y., Lu, Z., Lo, R., and Kuang, G.M. (2022). microRNA-145-5p inhibits prostate cancer bone metastatic by modulating the epithelial-mesenchymal transition. Front. Oncol. *12*, 988794.
43. Jiang, Y., Liu, J., Xu, H., Zhou, X., He, L., and Zhu, C. (2021). DAPK2 activates NF-κB through autophagy-dependent degradation of I-κBα during thyroid cancer development and progression. Ann. Transl. Med. *9*, 1083.
44. Karin, M. (2006). Nuclear factor-kappaB in cancer development and progression. Nature *441*, 431–436.
45. Xu, P., Cai, F., Liu, X., and Guo, L. (2015). Sesamin inhibits lipopolysaccharide-induced proliferation and invasion through the p38-MAPK and NF-κB signaling pathways in prostate cancer cells. Oncol. Rep. *33*, 3117–3123.
46. Yao, C., Li, G., Cai, M., Qian, Y., Wang, L., Xiao, L., Thaiss, F., and Shi, B. (2017). Prostate cancer downregulated SIRP-α modulates apoptosis and proliferation through p38-MAPK/NF-κB/COX-2 signaling. Oncol. Lett. *13*, 4995–5001.
47. Ochi, M., Nakasa, T., Kamei, G., Usman, M.A., and Mahmoud, E. (2014). Regenerative medicine in orthopedics using cells, scaffold, and microRNA. J. Orthop. Sci. *19*, 521–528.
48. Mei, L.L., Wang, W.J., Qiu, Y.T., Xie, X.F., Bai, J., and Shi, Z.Z. (2017). miR-145-5p Suppresses Tumor Cell Migration, Invasion and Epithelial to Mesenchymal Transition by Regulating the Sp1/NF-κB Signaling Pathway in Esophageal Squamous Cell Carcinoma. Int. J. Mol. Sci. *18*, 1833.
49. Schneider, C.A., Rasband, W.S., and Eliceiri, K.W. (2012). NIH Image to ImageJ: 25 years of image analysis. Nat. Methods *9*, 671–675.

CellPress
OPEN ACCESS

STAR★METHODS

KEY RESOURCES TABLE

REAGENT or RESOURCE	SOURCE	IDENTIFIER
Antibodies		
Rabbit monoclonal anti-COX-2	Cell Signaling Technology	Cat#12282; RRID: AB_2571729
Rabbit monoclonal anti-Cleaved Caspase-3	Cell Signaling Technology	Cat# 9661
Rabbit monoclonal anti-Cleaved Caspase-9	Cell Signaling Technology	Cat# 9501
Rabbit monoclonal anti-Caspase-3	Cell Signaling Technology	Cat# 14220; RRID:AB_2798429
Rabbit monoclonal anti-Caspase-9	Cell Signaling Technology	Cat#9502
Rabbit monoclonal anti-IKKα	Cell Signaling Technology	Cat#11930
Rabbit monoclonal anti-IKKβ	Cell Signaling Technology	Cat#8943
Rabbit monoclonal anti–pIKKα/β	Cell Signaling Technology	Cat#2697
Rabbit monoclonal anti-IκBα	Cell Signaling Technology	Cat#4814
Rabbit monoclonal anti-*p*-IκBα	Cell Signaling Technology	Cat#2859
Rabbit monoclonal anti-p50	Santa Cruz Biotechnology	Cat#sc-8414
Rabbit monoclonal anti-p65	Santa Cruz Biotechnology	Cat#sc-8008
Rabbit monoclonal anti-MAP3K11	Cell Signaling Technology	Cat#11934
β-actin	Cell Signaling Technology	Cat#4970; RRID: AB_2223172
Cytochrome *c*	Santa Cruz Biotechnology	Cat#sc-13560
Bax	Proteintech Group	Cat#50599-2-Ig
Bcl-2	Proteintech Group	Cat#12789-1-AP
Lamin B1	Proteintech Group	Cat#12987-1-AP
CDK4	Cell Signaling Technology	Cat#12790; RRID:AB_2631166
Cyclin D1	Cell Signaling Technology	Cat#55506; RRID:AB_2827374
MMP-2	Cell Signaling Technology	Cat#4022
MMP-9	Cell Signaling Technology	Cat#2270
E-Cadherin	Cell Signaling Technology	Cat#14472
N-Cadherin	Cell Signaling Technology	Cat#13116
PARP	Cell Signaling Technology	Cat#9542
Cleaved PARP	Cell Signaling Technology	Cat#5625; RRID:AB_10699459
Bacterial and virus strains		
pGL3-NFκB	Promega	Cat# E1791
Chemicals, peptides, and recombinant proteins		
Trillin	Pufei De Biotech Co., Ltd	14144-06-0
RPMI 1640 Medium	EallBio Biomedical Technology	03.4001C
DMEM	EallBio Biomedical Technology	03.1002C
Penicillin-Streptomycin	TransGen Biotech	P1400
Fetal Bovine Serum	VivaCell Biosciences	FBS-500
Lipofectamine 3000	Invitrogen	L3000001
Critical commercial assays		
Protein Quantification Kits	Thermo Fisher	23225
Protein Extraction Kits	Beyotime Co., Ltd.	P0027
CCK-8	MedChemExpress	HY-K0301
Apoptosis Detection Kits	MedChemExpress	HY-K1071
TRIzol	Invitrogen	15596026
Experimental models: Cell lines		
DU145	Procell Biological Company	CL-0231

(*Continued on next page*)

Continued

REAGENT or RESOURCE	SOURCE	IDENTIFIER
PC3	Cell Center of the Chinese Academy of Sciences	TCR-9
C4-2B	ATCC	CRL-3315
22RV1	Procell Biological Company	CL-0219
RWPE-1	ATCC	CRL-11609
Experimental models: Organisms/strains		
NYG immunodeficient mice	Liaoning Changsheng Biotechnology Co., Ltd.	N/A
Oligonucleotides		
COX-2 Forward TACCCTCCTCAAGTCCCTGA	GenePharma	N/A
COX-2 Reverse ACTGCTCATCACCCCATTCA	GenePharma	N/A
β-actin Forward GGCACCCAGCACAATGAA	GenePharma	N/A
β-actin Reverse TAGAAGCATTTGCGGTGG	GenePharma	N/A
miR-145-5p mimics Sequence GUCCAGU UUUCCCAGGAAUCCCU	GenePharma	N/A
miR-145-5p mimics Sequence AGGGAUU CCUGGGAAAACUGGAC	GenePharma	N/A
miR-145-5p inhibitor Sequence AGGGAU UCCUGGGAAAACUGGAC	GenePharma	N/A
MAP3K11 Forward GCCUUAGGAUAUUG CUGUUTT	GenePharma	N/A
MAP3K11 Reverse AACAGCAAUAUCCUA AGGCTT	GenePharma	N/A
U6 Forward AGAGAAGATTAGCATGGCCCCTG	GenePharma	N/A
U6 Reverse ATCCAGTGCAGGGTCCGAGG	GenePharma	N/A
Software and algorithms		
GraphPad Prism 9.0 software	GraphPad Prism Software Inc.	https://www.graphpad.com/
ImageJ	Schneider et al.[49]	https://imagej.net
Other		
target genes for miR-145-5p	PITA	https://genie.weizmann.ac.il/pubs/mir07/mir07_data.html
target genes for miR-145-5p	miRTarBase	http://mirtarbase.mbc.nctu.edu.tw/php/index.php
target genes for miR-145-5p	microT	https://dianalab.e-ce.uth.gr/html/dianauniverse/index.php?r=microT_CDS
target genes for miR-145-5p	TargetScan	https://www.targetscan.org/vert_80/
target genes for miR-145-5p	PicTar	https://pictar.mdc-berlin.de

EXPERIMENTAL MODEL AND STUDY PARTICIPANT DETAILS

Cell culture

Human prostate cancer cell lines DU145 and 22RV1 were obtained from Procell Biological Company (Wuhan, China), while C4-2B and RWPE-1 were sourced from the American Type Culture Collection (ATCC). PC3 cells were acquired from the Cell Center of the Chinese Academy of Sciences (Beijing, China). DU145 cells were cultured in DMEM medium, whereas PC3, 22RV1, C4-2B, and RWPE-1 cells were maintained in RPMI-1640 medium. Both media were supplemented with 1% penicillin-streptomycin and 10% fetal bovine serum (FBS). All cell lines were incubated at 37°C in a humidified atmosphere containing 5% CO_2.

Animal experiments

This animal study was conducted in accordance with the guidelines of the Dalian Medical University Animal Care and Ethics Committee (ethical approval number: AEE17030) and utilized male NYG immunodeficient mice (4–6 weeks old) sourced from the university's SPF Laboratory Animal Center. The mice were housed under controlled conditions. Each mouse received a subcutaneous injection of 1×10^7 DU145 cells in 100 μL of PBS into the right axillary fossa. Two weeks post-injection, the mice were divided into three

groups (n = 5 each) and treated daily for 14 days with either PBS (control), 10 mg/kg Trillin, or 20 mg/kg Trillin via intraperitoneal injections. Body weight and tumor volume were monitored bi-daily. After 30 days, the mice were euthanized, and tumors were harvested, weighed, and preserved in 10% formalin for paraffin embedding. Immunohistochemical staining of tumor tissues was performed to analyze COX-2 and MAP3K11 expression, which was observed using a Leica DM4 B fluorescence microscope. This study comprehensively assessed the therapeutic impact of Trillin on tumor growth and gene expression.

METHOD DETAILS

Cell viability assay

In this study, DU145, PC3, 22RV1, C4-2B, and RWPE-1 cells were seeded in wells at defined densities to achieve approximately 70% confluence. Following this, the cells were treated with a range of Trillin concentrations (0, 1, 5, 10, 25, and 50 μM). After incubation periods of 12, 24, or 48 h, 10 μL of CCK-8 reagent was added to each well, followed by an additional 2-h incubation. The absorbance was then measured at 450 nm using a microplate reader (Tecan, Switzerland). This process was repeated multiple times to determine the IC_{50} values for DU145 and PC3 based on the dose-response data collected at the 48-h mark.

Colony formation assay

DU145 and PC3 cells were initially seeded at 4,000 cells per well in six-well plates. Post-adherence, they were treated with Trillin at 0, 5, 10, and 20 μM for 48 h. Afterward, the medium was replaced with fresh one, and the cells were cultured until visible colonies formed. These colonies were then fixed with 4% paraformaldehyde, stained with 0.1% crystal violet, air-dried, and imaged, allowing for a detailed analysis of Trillin's effects.

Wound healing assay

DU145 and PC3 cells were grown in 6-well plates to form a confluent monolayer, followed by serum starvation for 6 h. A uniform wound was then created in the cell layer using a sterile pipette tip. The cells were treated with Trillin at concentrations of 0, 5, 10, and 20 μM in serum-free medium for 48 h. Images were taken at 0 and 48 h post-wounding with a Leica DMi1 microscope. Cell migration was assessed by analyzing five fields per wound, providing data on Trillin's effect on cell healing.

Transwell invasion assay

The matrix gel mixed with DMEM/1640 medium (1:10 ratio) is applied to an insert membrane and incubated at 37°C to solidify. DU145 and PC3 cells are prepared in serum-free medium with Trillin (0, 5, 10, 20 μmol/L), added to the upper chamber at a density of 5×10^5 cells/mL. The lower chamber receives DMEM/1640 medium with fetal bovine serum and Trillin. After 24 h, the upper chamber is cleared with a cotton swab, and the insert is fixed and stained with crystal violet. Post-washing, cells are imaged and counted under an inverted microscope.

Flow cytometry

In this flow cytometry protocol, DU145 and PC3 cells are cultured in 6 cm dishes and treated with Trillin at concentrations of 0, 5, 10, 20 μmol/L for 48 h. After treatment, cells are washed with PBS, trypsinized without EDTA, and centrifuged to collect. After two PBS washes, cells are resuspended in binding buffer and stained with Annexin V-FITC and Propidium Iodide, then incubated in darkness at room temperature for 15 min to assess apoptosis using a cytoflex flow cytometer. For cell cycle analysis, cells treated with Trillin are fixed in ice-cold 70% ethanol for 12 h at 4°C, then washed with ice-cold PBS, stained with propidium iodide solution, and incubated at 37°C in darkness for 30 min. The cell cycle is then analyzed using the cytoflex flow cytometer at a 488 nm wavelength.

Confocal immunofluorescence analysis

DU145 cells, seeded on coverslips, were treated with Trillin at 0, 10, and 20 μM for 48 h. Post-treatment, the cells were fixed using 4% paraformaldehyde and permeabilized with 0.2% Triton X-100. Blocking was performed with 5% BSA, followed by overnight incubation at 4°C with primary antibodies targeting cytochrome c, p50 or p65. This was succeeded by application of secondary antibodies conjugated with either fluorescein isothiocyanate or rhodamine isothiocyanate. DAPI was used for nuclear staining. Fluorescent imaging was conducted using a Leica DM4 B confocal microscope to visualize the antibody interactions.

Western blot

Proteins extracted from cell lysates or isolated through streptavidin-agarose pulldown assays were first separated on SDS-PAGE minigels and then transferred to PVDF membranes. These membranes were blocked using a 5% non-fat powdered milk buffer, followed by incubation with specific primary and secondary antibodies. Protein bands were detected through enhanced chemiluminescence (ECL) and their intensities were quantified using ImageJ software from the National Institutes of Health. Protein concentrations were ascertained using the BCA method.

qRT-PCR

Total RNA from DU145 and PC3 cells was extracted using Trizol and reverse transcribed with the Prime Script TM RT-PCR Kit (GENERAL Bio Inc, Anhui, China). Specific primers were utilized for amplifying cDNA for various genes, including COX-2, β-actin, miR-145-5p, its inhibitor, MAP3K11, and U6, sourced from GenePharma, Suzhou, China. The PCR products were analyzed on 1.5% agarose gels, visualized under UV light, and quantified. qRT-PCR analysis was conducted using an SYBR Green kit (Bio-Rad Laboratories, Inc., Hercules, CA, USA), and gene expression quantification was performed employing the 2-ΔΔCt method, with RNU6 (U6) serving as the internal standard in the experiments.

Cell transfection

In the cell transfection assays, DU145 and PC3 cells were seeded in 6-well plates at 5×10^5 cells/ml and transfected at ~80% confluence using Lipofectamine 3000. The cells were separately transfected with has-miR-145-5p NC, mimics, and inhibitors. For siRNA transfection, 4 μg of MAP3K11 was used per well for 48 h. Post-transfection, gene and protein expression levels were assessed through qRT-PCR or Western Blot.

Streptavidin-agarose pulldown assay

In this protocol, nuclear extract proteins 400 μg were interacted with a 400 μL mixture, comprising 4 μg of biotinylated DNA probe and 40 μL of streptavidin-conjugated agarose beads, in PBSi buffer (PBS with 1 mM EDTA, 1 mM DTT, and a protease inhibitor cocktail). This incubation occurred at room temperature over 5 h on a rotating shaker. Subsequent to the incubation, the beads were subjected to centrifugation for pellet formation, followed by dissociation in 50 μL of 2× Laemmli sample buffer. The dissociation process involved boiling at 100°C for 10 min. The resulting supernatant was then subjected to Western blot analysis for protein identification.

Dual-luciferase assay

In 293T cells, either the pGL3-NFκB plasmid or pGL3-Basic (negative control) is co-transfected in 6-well plates. Post-transfection, the cells are incubated at 37°C with 5% CO_2 for 24 h for optimal luciferase gene expression. Subsequently, they are treated with Trillin at 0, 5, 10 and 20 μmol/L concentrations for 48 h. The alterations in luciferase activity that ensue are quantified utilizing the Dual-Luciferase Reporter Assay System, and the firefly luciferase activity is normalized in reference to renilla luciferase activity.

Bioinformatics analysis of public database reanalysis

For expression analysis of miR-145-5p in prostate cancer and normal tissues or CRPC cell lines was referenced published article.[24,35,36] Additionally, analysis of miRNA-target gene interactions, five publicly available miRNA-mRNA databases were employed to predict potential target genes for miR-145-5p and ascertain common genes. These databases include PITA (https://genie.weizmann.ac.il/pubs/mir07/mir07_data.html), miRTarBase (http://mirtarbase.mbc.nctu.edu.tw/php/index.php), microT (https://dianalab.e-ce.uth.gr/html/dianauniverse/index.php?r=microT_CDS), TargetScan (https://www.targetscan.org/vert_80/) and PicTar (https://pictar.mdc-berlin.de). After intersecting the public databases, we identified seven target genes for mir-145-5p. Excluding three molecules not involved in inflammatory pathways, the remaining four were analyzed using the StarBase database for online analysis (https://rnasysu.com/encori/panCancer.php), all data used comes from TCGA. To use this resource, select "Gene Differential Expression," choose "PRAD" for the cancer type, and select the target gene (e.g., MAP3K11) to generate the relevant plots directly. Ultimately, MAP3K11 was selected for further validation. This approach provided a comprehensive exploration of miR-145-5p target genes while referencing these online resources for data integration.

QUANTIFICATION AND STATISTICAL ANALYSIS

The results from a minimum of three independent experiments are depicted as the mean ± standard deviation (SD). Prism 9 software and ImageJ[49] were used for analysis. Statistical significance between the control and treatment groups was assessed utilizing either one-way ANOVA or Student's t-tests, depending on the experimental design. Significance was established with a p-value less than 0.05. Asterisks were used to denote significance: one asterisk (*) for $p < 0.05$, two asterisks (**) for $p < 0.01$, and three asterisks (***) for $p < 0.001$.